Distinct trends in the speciation of iron between the shallow shelf seas and the deep basins of the Arctic Ocean

Thuroczy, C-E.; Gerringa, L. J. A.; Klunder, M.; Laan, P.; Le Guitton, M.; de Baar, H. J. W.

Published in:
Journal of geophysical research-Oceans

DOI:
10.1029/2010JC006835

Distinct trends in the speciation of iron between the shallow shelf seas and the deep basins of the Arctic Ocean

C.-E. Thuróczy,[1] L. J. A. Gerringa,[1] M. Klunder,[1] P. Laan,[1] M. Le Guitton,[2] and H. J. W. de Baar[1,3]

Received 27 November 2010; revised 20 May 2011; accepted 20 July 2011; published 13 October 2011.

[1] The speciation of iron was investigated in three shelf seas and three deep basins of the Arctic Ocean in 2007. The dissolved fraction (<0.2 μm) and a fraction < 1000 kDa were considered here. In addition, unfiltered samples were analyzed. Between 74 and 83% of dissolved iron was present in the fraction < 1000 kDa at all stations and depth, except at the chlorophyll maximum (42–64%). Distinct trends in iron concentrations and ligand characteristics were observed from the shelf seas toward the central deep basins, with a decrease of total dissolvable iron ([TDFe] > 3 nM on the shelves and [TDFe] < 2 nM in the Makarov Basin). A relative enrichment of particulate Fe toward the bottom was revealed at all stations, indicating Fe export toward the deep ocean. In deep waters, dissolved ligands became less saturated with Fe (increase of [Excess L]/[Fe]) from the Nansen Basin via the Amundsen Basin toward the Makarov Basin. This trend was explained by the reactivity of the ligands, higher (log alpha > 13.5) in the Nansen and Amundsen basins than in the Makarov Basin (log alpha < 13) where the sources of Fe and ligands were limited. The ligands became nearly saturated with depth in the Amundsen and Nansen Basins, favoring Fe removal in the deep ocean, whereas in the deep Makarov Basin, they became unsaturated with depth. Still here scavenging occurred. Although scavenging of Fe was attenuated by the presence of unsaturated organic ligands, their low reactivity in combination with a lack of sources of Fe in the Makarov Basin might be the reason of a net export of Fe to the sediment.

Citation: Thuróczy, C.-E., L. J. A. Gerringa, M. Klunder, P. Laan, M. Le Guitton, and H. J. W. de Baar (2011), Distinct trends in the speciation of iron between the shallow shelf seas and the deep basins of the Arctic Ocean, *J. Geophys. Res.*, *116*, C10009, doi:10.1029/2010JC006835.

1. Introduction

[2] Iron (Fe) is the fourth most abundant element (5% in weight) in the earth's crust [*Turner et al.*, 2001]. However, it is found at very low concentrations in seawater. This was due to oxygenation of the ocean during the early life evolution when photosynthetic microalgae appeared [*Turner et al.*, 2001; *de Baar and de Jong*, 2001], leading to massive precipitation of iron. Nowadays, Fe is such a scarce element, that it is limiting phytoplankton growth in 40% of the world ocean (High Nutrient, Low Chlorophyll (HNLC)) [*de Baar et al.*, 1990; *Martin et al.*, 1991; *de Baar and de Jong*, 2001].

[3] Despite its very low concentrations, Fe is essential for phytoplankton in euphotic zones of the surface ocean. It is used in enzymes and in vital processes in cells like photosynthesis [*Sunda et al.*, 1991; *Sunda*, 2001; *Timmermans et al.*, 2001, 2005]. Phytoplankton, which is the base of the food web in the ocean, is also responsible for fixation of dissolved carbon dioxide. Microbial communities such as bacteria and archaea also need Fe for their functioning [*Tortell et al.*, 1999]. These organisms are, in contrast to phytoplankton, present throughout the whole water column; *Reinthaler et al.* [2006] are responsible for degradation and remineralization of sinking organic matter.

[4] Dissolved Fe exists in seawater above concentrations determined by the solubility product of its oxy-(hydr)oxides [*Kuma et al.*, 1996; *Millero*, 1998] due to the presence of natural ligands. These ligands are mainly organics (Dissolved Organic Matter (DOM)) [*Hirose*, 2007] originated from living organisms, and bind up to 99.9% of Fe [*Gledhill and van den Berg*, 1994; *Rue and Bruland*, 1995; *Wu and Luther*, 1995; *Nolting et al.*, 1998; *Powell and Donat*, 2001; *Gerringa et al.*, 2006, 2007].

[5] The distribution of Fe is controlled by the competition between stabilization and removal processes and by the presence of external sources of Fe to the ocean [*de Baar and de Jong*, 2001]. Stabilization of Fe in seawater is ensured by organic complexation with natural ligands, which increases the residence time of Fe in seawater and hence enhances its

[1]Royal Netherlands Institute for Sea Research, Den Burg, Netherlands.
[2]Centre for Estuarine and Marine Ecology, Netherlands Institute for Ecology, Royal Dutch Academy of Sciences, Yerseke, Netherlands.
[3]Department Ocean Ecosystems, University of Groningen, Groningen, Netherlands.

0148-0227/11/2010JC006835

potential bioavailability. Iron can be removed from the water column by precipitation as oxy-hydroxides and by adsorption and scavenging on settling particles (>0.2 μm). Fine colloids are known to be very reactive [*Wells and Goldberg*, 1993; *Wells et al.*, 2000; *Nishioka et al.*, 2001, 2005] and can have a long residence time in seawater. These fine colloids can be the first step in the removal of Fe in the deep ocean by forming larger aggregates able to sink rapidly [*Kepkay*, 1994; *Logan et al.*, 1995; *Wu et al.*, 2001; *Cullen et al.*, 2006]. The main Fe sources in the Arctic Ocean are predominantly inputs from the Eurasian and Canadian rivers, sediment re-suspension occurring on the shelves and continental slopes, sea ice melting, upwelling and hydrothermal vents [*Measures*, 1999; *de Baar and de Jong*, 2001; *Moore and Braucher*, 2008; M. B. Klunder et al., Dissolved iron in the Arctic shelf seas and surface waters of the central Arctic Ocean: Impact of Arctic river water and ice-melt, submitted to *Journal of Geophysical Research*, 2011a; M. B. Klunder et al., Dissolved Fe in the Arctic Ocean: Important role of hydrothermal sources, shelf input and scavenging removal submitted to *Journal of Geophysical Research*, 2011b]. Aerosols deposition to the surface Arctic Ocean is not a major source of Fe [*Moore and Braucher*, 2008] as also detailed by Klunder et al. (submitted manuscript, 2011a, 2011b).

[6] The Arctic Ocean is a relatively enclosed ocean, surrounded by lands, and has restricted connections with the Atlantic and Pacific Oceans via the Fram Strait (approximately 2500 m deep) and the Bering Strait (approximately 40 m deep), respectively. The Arctic Ocean plays a key role in the deep water formation, where cold and saline Arctic water sinks contributing to the thermo-haline circulation around the globe. The Arctic Ocean is threatened by quick climate change, with melting of sea ice due to global warming which directly affects its seasonal variations and life cycles, such as phytoplankton blooms. Therefore it is an interesting environment which needs to be investigated before and during major changes take place.

[7] The Eurasian shelf seas (Figure 1), mainly composed by the Barents Sea, the Kara Sea, the Laptev Sea, the East Siberian Sea and the Chukchi Sea, represent nearly 70% of the surface of the Arctic Ocean [*Tomczak and Godfrey*, 1994]. These shallow areas (10–350 m depth) are strongly influenced by freshwater inputs from the Eurasian and Canadian rivers [*Guay and Falkner*, 1997]. Four major deep basins compose the deep Arctic Ocean: the Nansen Basin, the Amundsen Basin, the Makarov Basin and the Canadian Basin (Figure 1), all separated by ridges.

[8] This study aimed to investigate the speciation of Fe at several locations of the Arctic Ocean, which are very different in terms of geographical situation, water depth and external influences. With this aim, seven stations were sampled during the ARK XXII/2 cruise on board R/V *Polarstern* in 2007 (Figure 1); three stations were taken in different seas of the Eurasian continental shelves (Barents Sea, Kara Sea and Laptev Sea), one was chosen on the continental slope of the Nansen Basin, and three were taken in deep basins (Nansen, Amundsen and Makarov basins, Figure 1). Three different size-fractions were considered in this study: (1) unfiltered samples (UNF, which contains the particulate fraction > 0.2 μm and the dissolved fraction < 0.2 μm); (2) the dissolved fraction (consisting of a truly dissolved fraction and of several colloidal pools [*Nishioka et al.*, 2005, *Thuróczy et al.*, 2010; *Boye et al.*, 2010]); and (3) the fraction smaller than 1000 kDa which contains the fine colloids and the truly soluble phase. The knowledge of Fe concentrations and ligand characteristics in different sizes-fractions will provide valuable information to explain the processes controlling stabilization of Fe via organic complexation versus removal of Fe via precipitation and scavenging of Fe; and hence better understand the cycle of Fe in the oceans.

[9] This work was part of the GEOTRACES program [*Scientific Committee on Oceanic Research*, 2006]. The distribution of dissolved Fe (DFe) over the whole water column was investigated on the same cruise (Klunder et al., submitted manuscript, 2011a, 2011b). In addition to that, other trace elements were analyzed during this expedition like dissolved aluminum and manganese as tracers of Fe sources [*Middag et al.*, 2009].

2. Material and Methods

[10] Analyses of Fe, ligand concentrations and conditional stability constant K′ were done in each of the three size-fractions: (1) the unfiltered samples (UNF), comprising the particulate fraction (>0.2 μm) and the dissolved fraction (<0.2 μm, note that from the particulate fraction, minerals and refractory material do not participate in the speciation of Fe, and that Fe concentrations from UNF samples corresponds to total dissolvable Fe (TDFe, for more details, see sections 2.3.2 and 4)), (2) the dissolved fraction (<0.2 μm), and (3) the fraction < 1000 kDa, comprising the truly soluble and the small colloidal fractions. Note that the fraction comprised between 1000 kDa and 0.2 μm is called larger colloidal fraction in the present study.

2.1. Cleaning Procedures

[11] All sample bottles (Nalgene, Low-Density Polyethylene, LDPE, 60 to 1000 mL) were treated following a 3 steps cleaning procedure (detergent solution, 6 M HCl and 3 M nitric acid) in 60°C bath. Finally, the bottles were stored filled with 0.2 M 3QD-HNO_3 (3times quartz distilled from 65% reagent grade, J.T. Baker). Rinsings in between cleaning steps were done with MQ water (Millipore Milli-Q deionised water, R > 18.2 MΩ cm^{-1}).

2.2. Sampling and Filtrations

[12] Samples for Fe and ligand characteristics were collected in the Arctic Ocean during the ARK XXII/2 cruise (28 July–7 October 2007, Figure 1) on-board the German Research Vessel *Polarstern*. Three shelf sea stations were sampled: one in the Barents Sea (St. 239), one in the Kara Sea (St. 279), and one in the Laptev Sea (St. 407). Moreover, four deep stations were sampled: two in the Nansen Basin (St. 255 and 260), one in the Amundsen Basin (St. 309) and one in the Makarov Basin (St. 352).

[13] Samples were collected using the ultra-clean Titan Mk.II sampling system [*de Baar et al.*, 2008], which consists of an all-titanium frame on which 24 internally Teflon coated PVC GO-FLO samplers (General Oceanics Inc., volume 12 L) were attached. The frame was lowered using a Kevlar hydro-wire in areas freed of sea ice (open cracks).

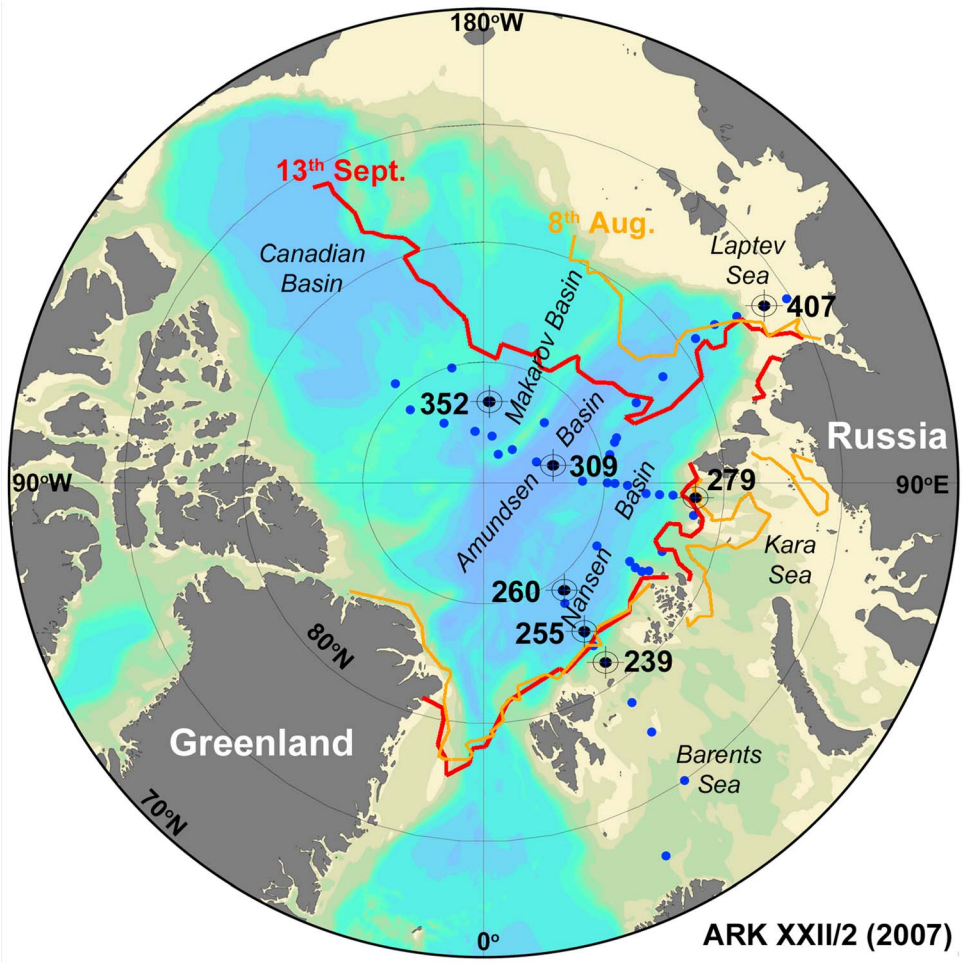

Figure 1. Chart of the Arctic Ocean with the stations sampled during the ARK XXII/2 cruise. Black target dots represent the 7 stations sampled for this study: St. 239 in the Barents Sea (80°59.6′N-33°59′E); St. 255 on the slope of the Nansen Basin (82°30.2′N-33°57.1′E); St. 260 in the Nansen Basin (84°29.5′N-36°6.9′E); St. 279 in the Kara Sea (81°12.3′N-81°12.3′E); St. 309 in the Amundsen Basin (87°1.9′N-104°56.7′E); St. 352 in the Makarov Basin (86°38.3′N-177°33.3′E) and St. 407 in the Laptev Sea (76°10.8′N-122°7.7′E). Blue dots are stations sampled with the titanium frame for trace element analyses. The orange line corresponds to the sea ice extend on the 8 August and the red line to the sea ice extend on the 13 September 2007.

Once back on deck it was directly placed in a clean-air laboratory container designed for the titanium frame.

[14] Unfiltered samples were taken first (Figure 2, step 1), the remaining seawater was directly filtered in-line (0.2 μm pore size filter, Sartorius Sartobran-300) using N_2 overpressure (1.5 atm) (Figure 2, step 2). All samples were collected in acid-cleaned LDPE bottles after fivefold rinsing of the bottles with the sample itself. Samples taken for analysis of Fe speciation were stored at 4°C when their analysis could be performed within 2 days; otherwise they were immediately frozen at −20°C in the dark. Ultrafiltration of the 0.2 μm filtered water (Figure 2, step 3) was performed immediately after sampling in a clean laminary flow bench. The filters were hollow fiber filters (Sterapore, Mitsubishi-rayon Co., Ltd.) with a size cut-off of 1000 kDa [*Nishioka et al.*, 2001]. A 12-channels peristaltic pump (ISM 937, Ismatec, IPC-N) with Tygon® LFL (Long Flex Life) tubing was used for the ultra-filtration with a flow rate of 7 mL.min^{-1}. The polyethylene hollow fiber filters were activated and cleaned in the home laboratory before use on board according to the protocol described by *Thuróczy et al.* [2010] and adapted from *Nishioka et al.* [2001]. Mass balance verification for Fe as well as for the ligands was done successfully with samples from the Southern Ocean [*Thuróczy et al.*, 2010].

2.3. Analytical Procedures

2.3.1. Iron Analyses

[15] Shipboard analysis of samples in the dissolved (DFe, <0.2 μm) and <1000 kDa ($Fe_{<1000\ kDa}$) fractions was done by an in-line Flow Injection Analysis system using chemiluminescence as detection method [*de Jong et al.*, 1998; *de Baar et al.*, 2008] and is described in detail by *Klunder et al.* [2011]. The UNF samples (for TDFe) were stored acidified (pH 1.8) for 1 year before being analyzed in the home laboratory using the same method and system as described above. Standard deviations of the duplicate measurements (dissolved fraction) or triplicate measurements (fraction

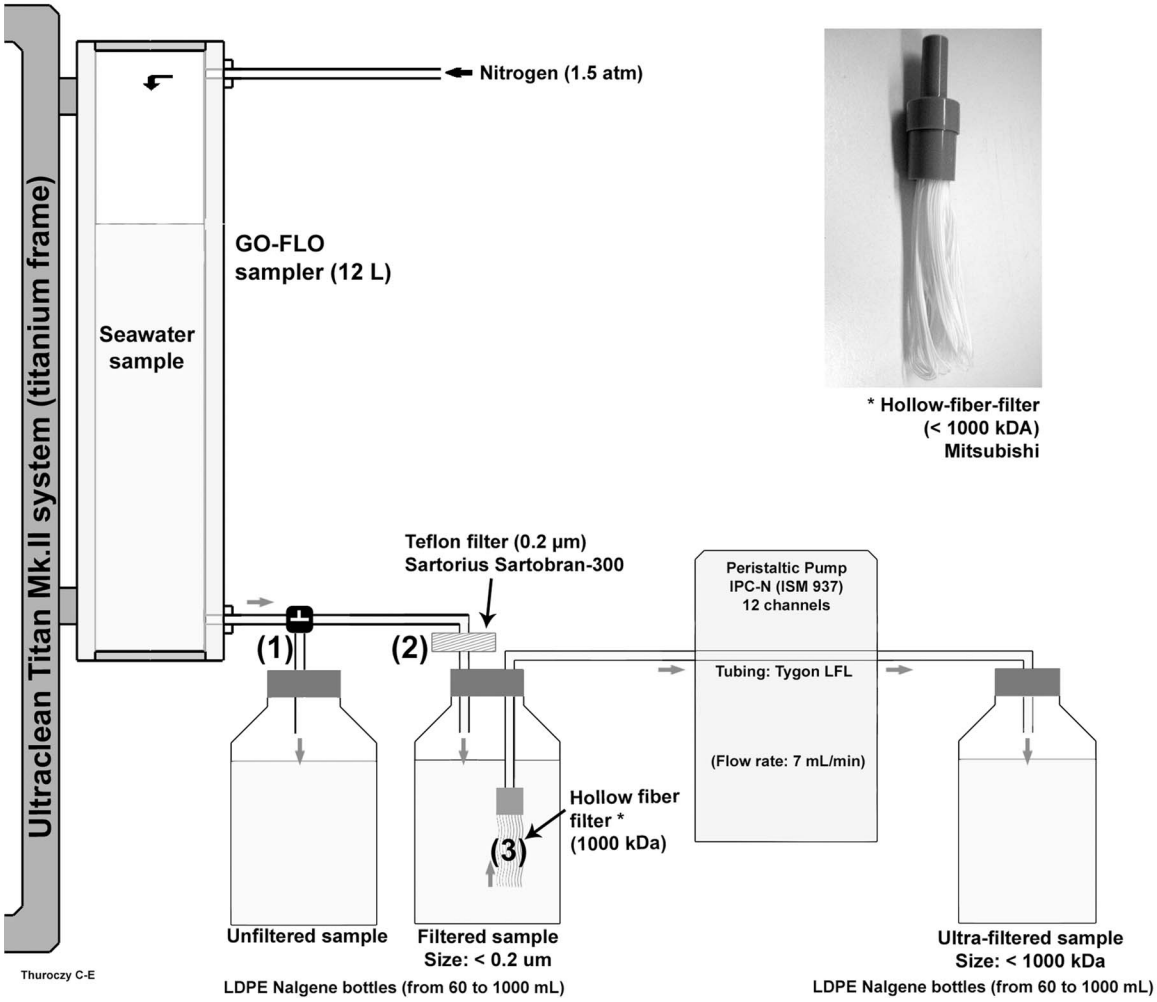

Figure 2. Size-fractionation of seawater. (1) Unfiltered sampling. (2) Filtration of seawater sample over 0.2 μm pore size filter. (3) Ultra-filtration of the seawater sample over 1000 kDa pore size filter. Steps 1 and 2 were done in the titanium-frame clean air container. Step 3 was performed in a laminary flow bench (class 0) in another clean room.

<1000 kDa and UNF samples) of one sample were less than 5%.

2.3.2. Iron Speciation: Sample Treatment, Voltammetric Procedure, and Calculations

[16] Organic complexation of Fe was determined by Competing Ligand Exchange - Adsorptive Stripping Voltammetry (CLE-AdSV) using 2-(2-Thiazolylazo)-p-cresol (TAC, 10 μM) as a competing ligand [*Croot and Johanson*, 2000]. Seawater was buffered to pH 8.05 by adding a mixed NH_3/NH_4OH borate buffer (final concentration 5 mM). The equipment, voltammetric procedures, samples and chemicals preparations are described by *Thuróczy et al.* [2010].

[17] Total ligand (Lt) concentrations, conditional stability constants K′ and their respective standard deviations were calculated using the Langmuir model [*Gledhill and van den Berg*, 1994] applying the nonlinear regression of the Langmuir isotherm [*Gerringa et al.*, 1995]. By using the Langmuir model it is assumed that equilibrium between all Fe(III) species exists, all binding sites between Fe and the unknown ligand L are equal and that the binding is reversible. The equations for the calculation of Fe speciation are described by *Thuróczy et al.* [2010]. The ligand (L) characteristics were estimated assuming the presence of one ligand pool. Ligand concentrations [Lt] are in Equivalent of nano-molar Fe (Eq of nM Fe). The sensitivity S (in Amper. mol^{-1}) of the method is influenced by ligand sites not yet saturated with Fe as explained by *Turoczy and Sherwood* [1997] and *Hudson et al.* [2003]. This is accounted for by an algebraic solution of the equilibrium equations including the Langmuir isotherm, in which S is determined together with Lt and K′. The parameters S, Lt, and K′ are given with the standard deviation of the fit of the model to the data.

[18] Concentrations of ligands in the dissolved fraction (<0.2 μm) and in the fraction < 1000 kDa were calculated using the concentration of Fe from the same size-fractions. However, for the UNF samples, the concentrations of Lt and Excess L were estimated in two ways: an upper limit using [TDFe] and a lower limit using [DFe] in the calculations. The reason is that part of Fe in UNF samples is refractory (unknown percentage) and does not participate in the complexation with natural organic ligands. Under natural conditions (seawater pH ~8), part of Fe is irreversibly bound

in colloids or into mineral particles which are refractory (not dissolvable); and, in UNF samples the presence of phytoplankton cells and microorganisms containing Fe, which is released in seawater after acidification, leads to an overestimation of the Fe concentration in the sample. The ligand concentration [Lt] and K′ are variables which depend on the Fe concentration used in the calculations and are thus artificially increased when using [TDFe] concentrations (assumed to be exchangeable for the calculations). However, the concentrations of Excess L ([Lt] - [Fe]), are hardly influenced by the Fe concentration [*Thuróczy et al.*, 2010].

[19] The first voltammetric analyses (St. 239 in the Barents Sea) showed interferences due to vibrations of the ship while breaking sea ice since the laboratory container, in which the analyses were performed, was placed in the bow of the ship. This resulted in large standard deviations of the ligand characteristics at this station. In order to avoid these disturbances further analyses were performed in the middle of the ship with a soft mattress placed under the mercury drop electrode.

2.3.3. Temperature, Salinity, Dissolved Oxygen, Fluorescence, and Light Transmission

[20] Temperature, conductivity (salinity), dissolved oxygen ($ml.l^{-1}$) and fluorescence (given in arbitrary units, a.u.) were measured from the CTD systems (Sea Bird SBE 911+) installed on the titanium frame. Light transmission (in percentage, %) was measured by the transmissiometer (SN 946) installed on the sampling system from the Alfred Wegener Institute (AWI) at the same stations studied here but at different casts.

[21] Vertical profiles of temperature, salinity and dissolved oxygen are shown in the auxiliary material.[1]

3. Results

3.1. Sea Ice Conditions, Hydrography, Fluorescence, and Light Transmission

[22] In winter the Arctic Ocean is completely covered by sea ice, which partly melts during spring and summer. Between the end of July 2007 (start of the cruise) and the end of August 2007, the sea ice extent severely decreased in the south part of the Amundsen and Makarov basins and in the Kara Sea (Figure 1). At the time of sampling, the stations in the Barents Sea and in Laptev Sea were ice-free (St. 239 and 407, respectively). At St. 279 in the Kara Sea, approximately 50% of the sea-surface was covered by sea ice. At the other stations (St. 255, 260, 309, and 352) the sea-surface was totally covered with a relatively thick layer of ice.

[23] Different water masses of the Arctic Ocean can be distinguished as shown in potential temperature versus salinity plots (θ/S diagrams, Figure 3). The Surface Water (SW) from the surface to 100–150 m depth has negative temperatures (<0°C) and salinities below 34.5. It is influenced by melted sea ice and river inputs. The distinction between sea ice melt and river input is explained by Klunder et al. (submitted manuscript, 2011a, 2011b) for the present study. *Yamamoto-Kawai et al.* [2005] could also distinguish the influence of sea ice and and river fresh water in the Arctic Ocean using δ18O and alkalinity. The Atlantic Water (AW), flowing eastward along the slope of the Eurasian continental shelves at approximately 100–900 m depth, is characterized by positive temperatures (>0°C) and salinities between 34.5 and 35 (Figure 3). Below the AW, the Eurasian Basin Deep Water (EBDW) is found (below 800 m). The EBDW comprises the Arctic Intermediate Water (AIW) found at around 800–2000 m and the Cold Bottom Water (CBW) below 2000 m depth. The AIW and CBW have negative temperatures and salinities above 34.8 (Figure 3). The CBW with temperatures below −0.9°C is present in the Nansen and Amundsen basins (Figure 3). In the Makarov Basin, the deep water has different properties (temperatures between −0.6 and 0°C) and is called the Deep Makarov Basin Water (DMBW). The DMBW is influenced by water derived from the Pacific Ocean, which is characterized by concentrations of silicate higher than 10 μM [*Anderson et al.*, 1994]. Details about the hydrography of the Arctic basins were described by *Anderson et al.* [1994] and *Rudels et al.* [2000].

[24] Fluorescence (Figure 4) corresponds to chlorophyll-a content and is an indicator of phytoplankton abundance [*Kiefer*, 1973; *Babin et al.*, 1996]. At St. 407 in the Laptev Sea, the signal was saturated due to the presence of a great amount of suspended material; therefore the data is not shown here. In the Barents Sea (St. 239) and in the Kara Sea (St. 279) the fluorescence was high (1.5 and 0.8 a.u., respectively). The other stations had a lower fluorescence signal, below 0.5 a.u.

[25] Low light transmission (Figure 4) was found at the surface where fluorescence was high. In the Barents Sea (St. 239) and in the Kara Sea (St. 279) lower light transmission was measured at the chlorophyll maximum (85% and 88%, respectively). In the deep basins, light transmission was relatively constant below 200 m depth, between 91 and 92%. Near the seafloor, light transmission was often lower due to the influence of sediments re-suspension.

3.2. Iron Concentrations

[26] The concentrations of TDFe (Figure 5 and Table 2a) varied between 0.7 and 63 nM. The very high concentrations were measured at shelf seas stations (up to 63 nM Fe at St. 239 and up to 11.9 nM Fe at St. 279) and above the slope of the Nansen Basin (St. 255) between 500 and 1200 m depth where [TDFe] was maximum (18 nM) 100 km away horizontally from the bottom slope. In surface waters (SW), average [TDFe] was 0.82 nM ± 0.18 (n = 2) in the Nansen Basin (St. 260), 2.42 nM ± 0.04 (n = 2) in the Amundsen Basin (St. 309), and 1.60 nM ± 0.02 (n = 2) in the Makarov Basin (St. 352). In the layer influenced by the AW, average [TDFe] were 1.74 nM ± 0.35 (n = 2), 1.88 nM ± 0.11 (n = 2), and 1.50 nM ± 0.56 (n = 2) in the same basins, respectively. Finally, below 800 m depth (AIW and CBW), average [TDFe] were 4.57 nM ± 0.67 (n = 4), 3.35 nM ± 0.63 (n = 5), and 1.57 nM ± 0.10 (n = 4) in the Nansen, Amundsen, and Makarov basins, respectively.

[27] The concentration of DFe (Figure 6a and Table 1) ranged from 0.17 to 1.52 nM. At the shelf sea stations [DFe] were relatively high and constant with depth; average [DFe] were 0.55 nM ± 0.29 (n = 5) in the Barents Sea (St. 239) and 0.91 nM ± 0.26 (n = 6) in the Kara Sea (St. 279) with a respective maximum of 1.0 and 1.3 nM Fe below the chlorophyll maximum. In the Laptev Sea (St. 407), average

[1] Auxiliary materials are available in the HTML. doi:10.1029/2010JC006835.

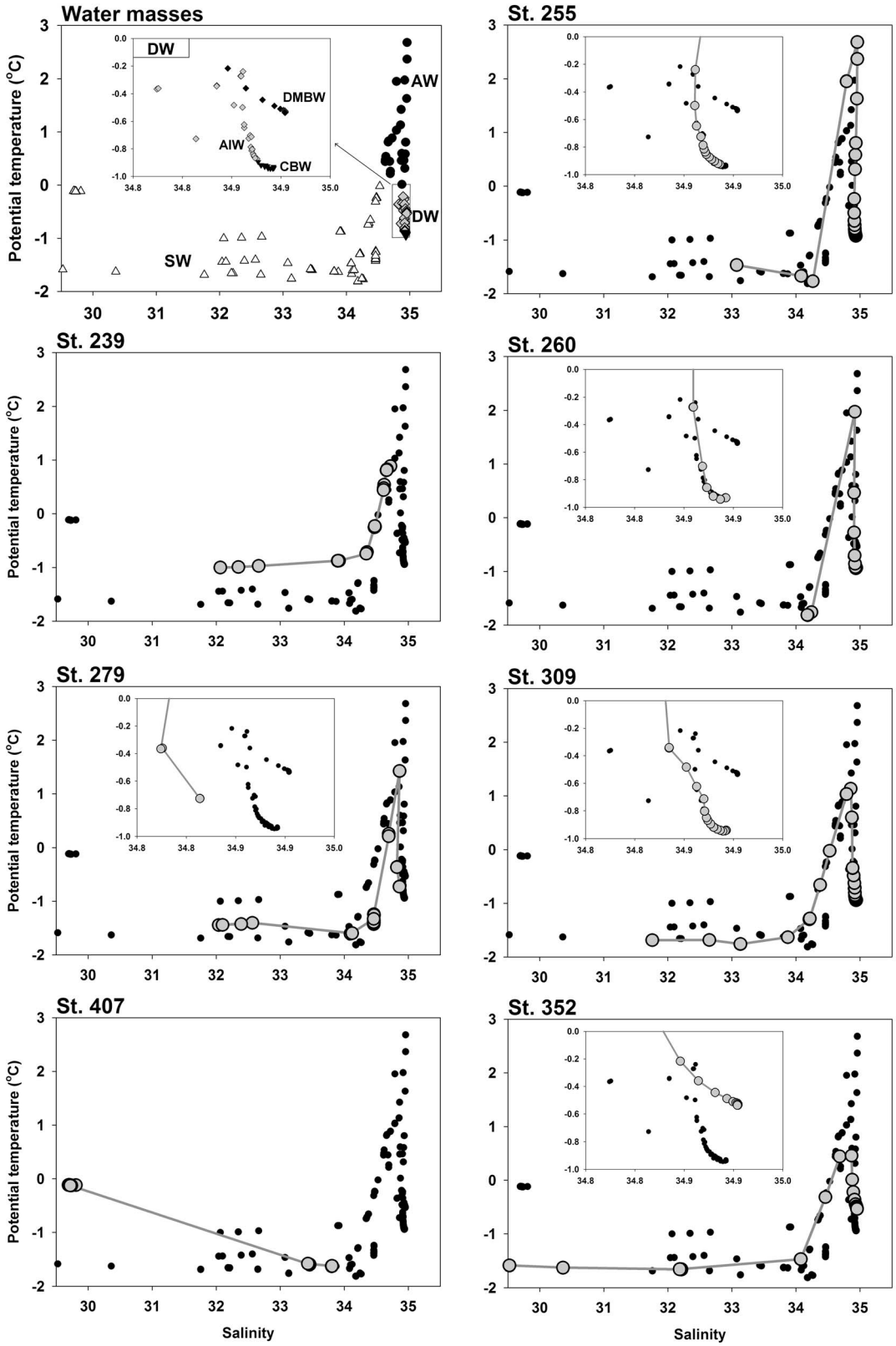
Water masses
DW
DMBW
AIW
CBW
AW
DW
SW
St. 255
St. 239
St. 260
St. 279
St. 309
St. 407
St. 352
Potential temperature (°C)
Salinity

Figure 3

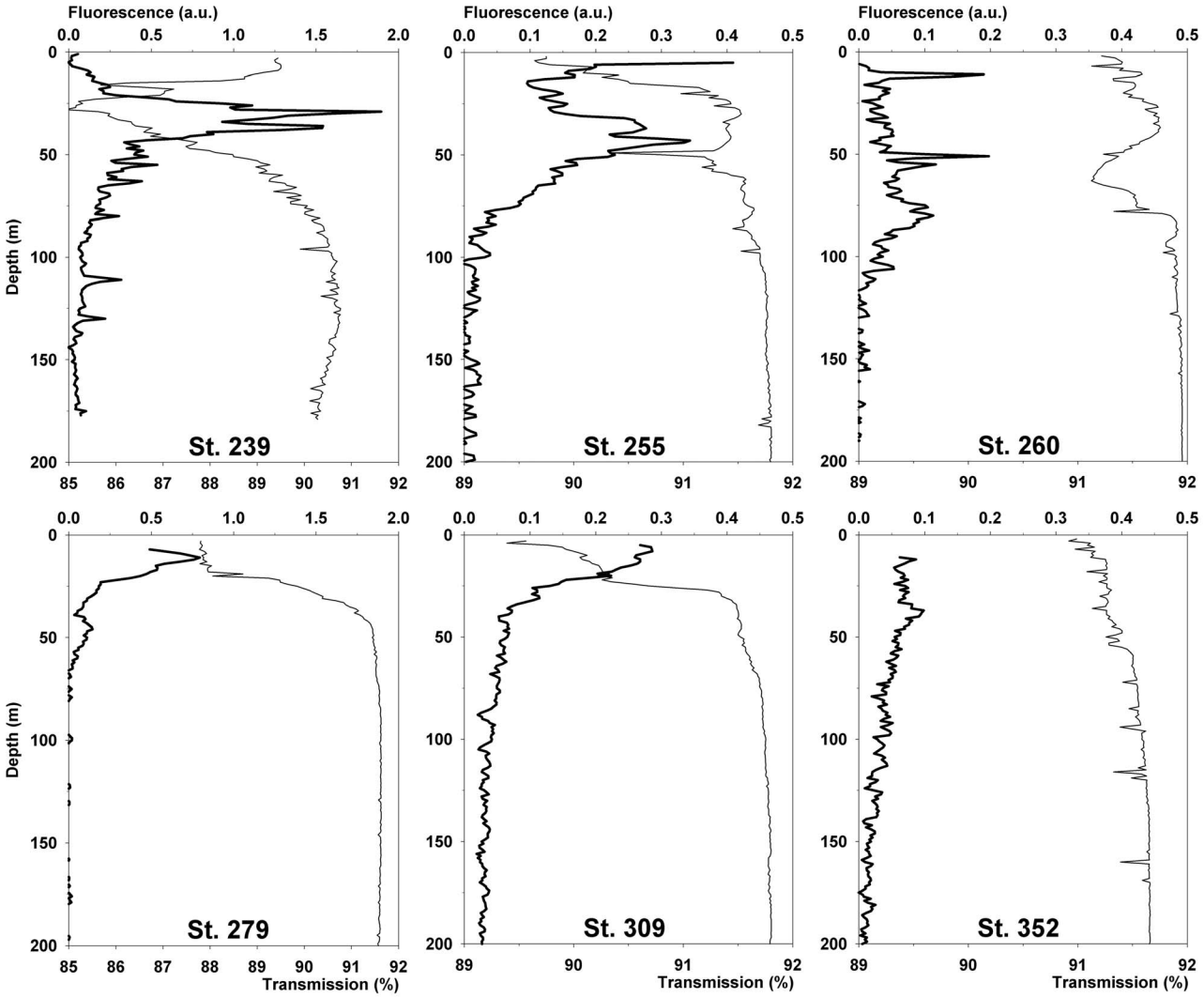

Figure 4. Fluorescence (a.u., top axis, thick line) and light transmission (%, bottom axis, thin line) in the upper 200 m at 6 stations sampled. Note the different scales for the fluorescence and for the light transmission between the shelf seas (left side: St. 239 in the Barents Sea and St. 279 in the Kara Sea) and the deep basins (St. 255 on the slope of the Nansen Basin; St. 260 in the Nansen Basin; St. 309 in the Amundsen Basin and St. 352 in the Makarov Basin).

[DFe] was 0.88 nM ± 0.21 (n = 3). In the Nansen Basin (St. 255 and 260), [DFe] increased from 0.31 and 0.27 nM Fe respectively at the surface, to 1.30 and 0.95 nM Fe at 2100 and 2500 m depth. In the deepest sample, [DFe] were lower, with 0.86 and 0.64 nM Fe, respectively. Conversely, in the Amundsen Basin (St. 309), [DFe] decreased steeply from 1.44 at the surface to 0.22–0.32 nM Fe at depth; and a same trend was observed in the Makarov Basin (St. 352) with a decrease of [DFe] from 1.52 nM Fe at surface to 0.17–0.22 nM Fe at depth. The detailed distribution of DFe from the same cruise is presented by Klunder et al. (submitted manuscript, 2011a, 2011b).

[28] The concentration of Fe in the fraction < 1000 kDa ([$Fe_{<1000\ kDa}$], Figure 6a and Table 1) accounted for

Figure 3. Potential temperature/Salinity diagram (θ/S) for the 7 stations sampled. In the top left graph the corresponding water masses present at the 7 stations are indicated, with the deep waters in the enlarged box. SW: Surface Water; AW: Atlantic Water; DW: Deep Water; AIW: Arctic Intermediate Water; CBW; Cold Bottom Water; DMBW: Deep Makarov Basin Water. The other graphs show the results of the separate stations with a gray line and large gray dots; the small black dots represent the 6 other stations for comparison. On the left side, the shelf sea stations (St. 239 in the Barents Sea; St. 279 in the Kara Sea and St. 407 in the Laptev Sea); on the right side, the deep basins (St. 255 on the slope of the Nansen Basin; St. 260 in the Nansen Basin; St. 309 in the Amundsen Basin and St. 352 in the Makarov Basin). When deep waters are present, they are shown in enlarged boxes. The vertical distribution of temperature and salinity is available in the auxiliary material.

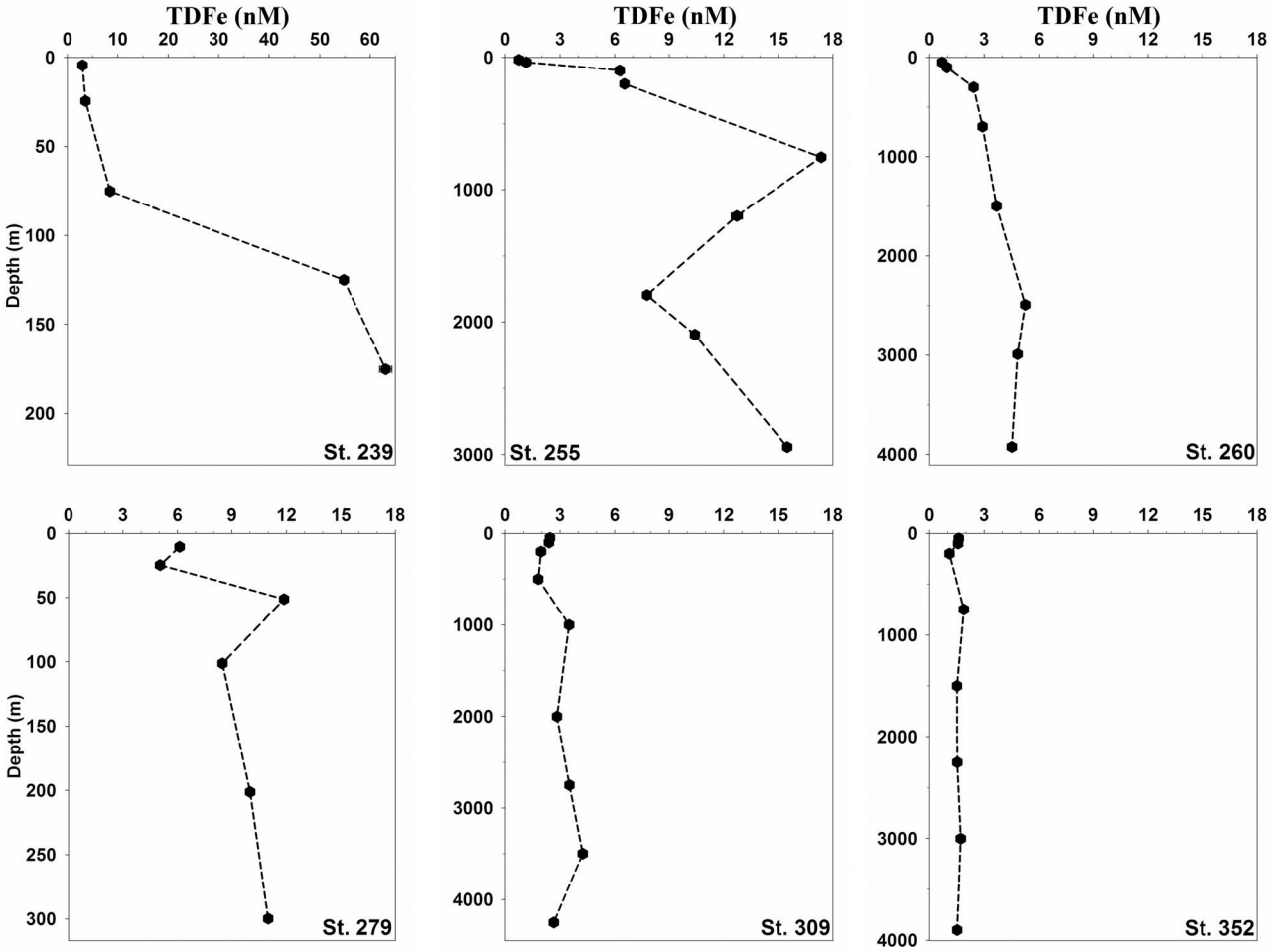

Figure 5. TDFe concentrations (nM, ±standard deviation of triplicate measurements) from unfiltered samples (with depth at 6 stations sampled. Shelf sea stations are on the left side. The depth axes are extended until the bottom depth: St. 239 at 229 m (Barents Sea); St. 255 at 3078 m (Nansen Basin slope); St. 260 at 4109 m (Nansen Basin); St. 279 at 317 m (Kara Sea); St. 309 at 4449 m (Amundsen Basin); St. 352 at 4005 m (Makarov Basin). Note the different scales for the concentrations at St. 239 (0–65 nM). Error bars are too small (<5%) to be seen on the graphs.

approximately 74 to 83% of the concentration of Fe in the dissolved fraction in the whole water column. Exceptions were the samples taken from the chlorophyll maximum, where 42 to 64% of DFe was present in the fraction < 1000 kDa.

3.3. Ligand Characteristics

[29] The ligands in the dissolved and <1000 kDa fractions were always found in excess with respect to the Fe concentrations (Tables 1, 2a, and 2b and Figure 7). At St. 239 in the Barents Sea, [$Lt_{<0.2\ \mu m}$] were higher (4.54 Eq of nM Fe ± 0.14, n = 3) between 25 and 125 m depth compared to the surface (5 m, 2.75 Eq of nM Fe) and deepest samples (175 m, 2.51 Eq of nM Fe). In the fraction < 1000 kDa the ligand concentrations were, as expected, lower than in the dissolved fraction and [$Lt_{<1000\ kDa}$] was relatively constant with depth (2.80 Eq of nM Fe ± 0.37 n = 5). However, the Kara Sea (St. 279) was an exception since below 25 m depth the ligand concentrations <1000 kDa were higher than in the fraction <0.2 μm. No contamination was seen here (Table 1) and each sample was filtered with a different filter to avoid cross contamination. The 5 samples where [$Lt_{<1000\ kDa}$] > [$Lt_{<0.2\ \mu m}$] appeared to be correct (see discussion). Filtration could cause disequilibrium in seawater by removal of constituents. One possible reason is that the smallest and most reactive fraction [*Nishioka et al.*, 2001, 2005; *Cullen et al.*, 2006] could have exchanged Fe during filtration and/or colloids or colloid aggregates might break and/or disperse during filtration, increasing the active surface and leading to disequilibrium between Fe and ligands in the filtrate (here <1000 kDa). The results from the Laptev Sea (St. 407) are reported in Table 1 but not in Figure 7, because of the limited number of samples. Here [$Lt_{<0.2\ \mu m}$] were above 2 Eq of nM Fe and [$Lt_{<1000\ kDa}$] were below 2 Eq of nM Fe. A maximum was measured in both dissolved and <1000 kDa fractions (between 2.3 and 3.1 Eq of nM Fe). In the deep basins, distinct maxima in [$Lt_{<0.2\ \mu m}$] and in [$Lt_{<1000\ kDa}$] were measured. At the slope of the Nansen Basin (St. 255) a maximum in the ligand concentration existed at 100–200 m depth with 5.2 Eq of nM Fe in the dissolved fraction. At St. 260 in the Nansen Basin and St. 309 in the Amundsen Basin, a maximum was measured in

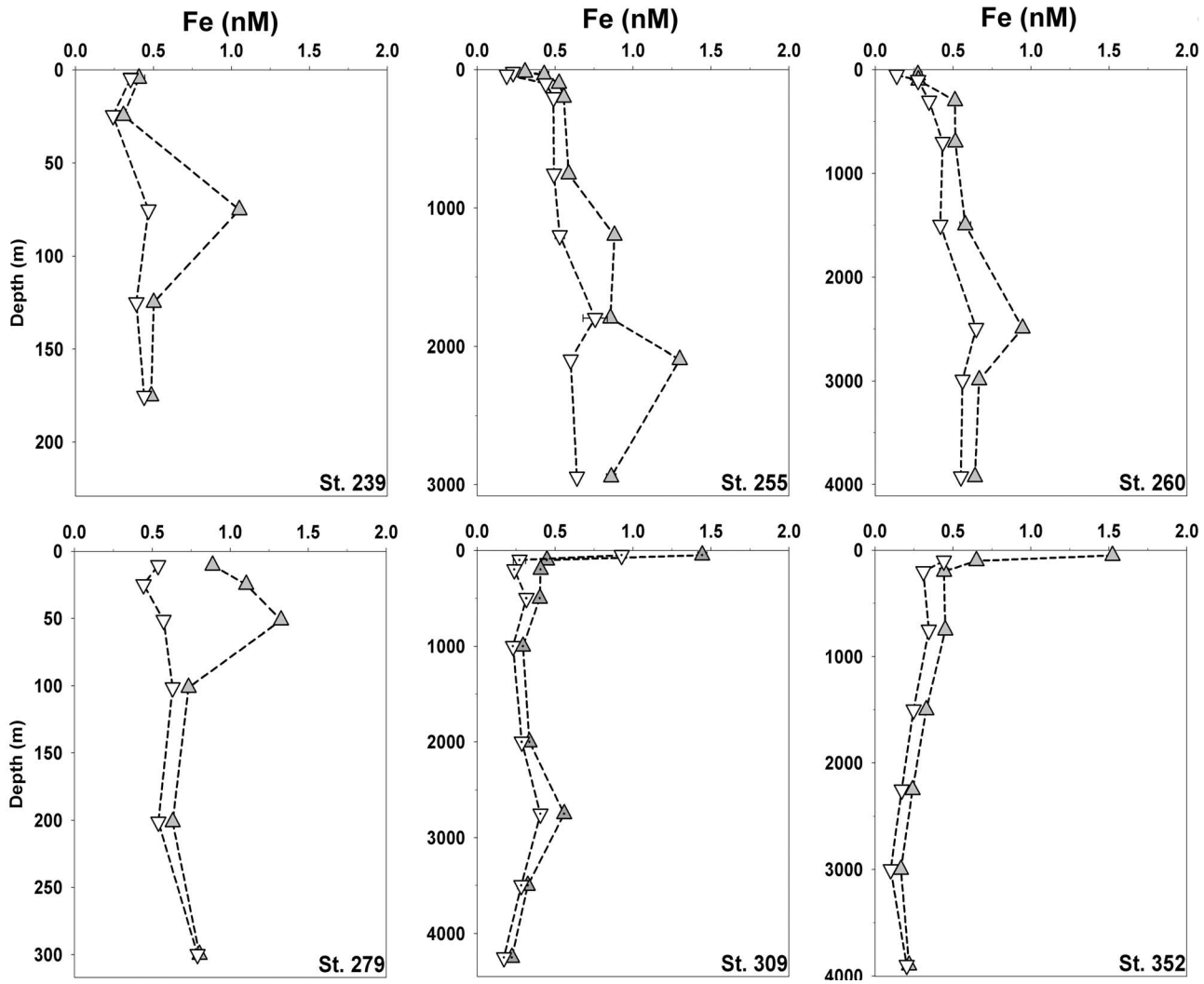

Figure 6a. Concentrations of Fe with depth at 6 stations sampled (same as in Figure 5) and for 2 size fractions: Dissolved fraction (<0.2 μm, gray triangles upwards looking) and fraction < 1000 kDa (white triangles downward looking). Fe concentrations are in nM (±standard deviation of duplicate or triplicate measurements). Error bars for Fe concentrations are too small (<5%) to be seen on the graphs. Shelf sea stations are on the left side. The depth axes are extended until the bottom depth.

both dissolved and <1000 kDa fractions (between 2.6 and 2 Eq of nM Fe and 3.5 and 2.1 Eq of nM Fe, respectively). In the Amundsen Basin (St. 309) a second maximum was observed in the dissolved fraction with 2.1 Eq of nM Fe at 2750 m depth. The Makarov Basin (St. 352) also had 2 maxima in the dissolved fraction but at different depths (Figure 6b): one at the surface (2.08 Eq of nM Fe) and one between 750 and 1500 m depth (2.16 Eq of nM Fe).

[30] Excess L expresses the binding potential of the ligands by showing the empty sites without relation to the parameter for which these sites are used. Trends with depth of Excess L were relatively similar to trends in total ligand concentrations (Figure 7 and Table 1). Excess L in the UNF fraction followed Excess L in the smaller fractions (within the analytical uncertainty). At St. 255 and 260 in the Nansen Basin, much larger Excess L in the UNF fraction were observed at the surface where they were minimal in the dissolved and <1000 kDa fractions. In the deep Makarov Basin (at 1500 and 2250 m depth) Excess L concentrations in the UNF fraction were lower (0.3 Eq of nM Fe) than Excess L in the dissolved fraction.

[31] The conditional stability constant K′ (Tables 1, 2a, and 2b) reflects the binding strength of the natural ligands with Fe. The K′ values in all fractions were relatively constant or increased slightly with depth. Average of K′ values in the fraction < 1000 kDa were $10^{21.96} \pm 0.36$ (n = 43) and in the dissolved fraction $10^{21.86} \pm 0.35$ (n = 45). The differences between the K′ values in the fraction < 1000 kDa and those in the dissolved fraction were not significant even if they were often found slightly higher in the fraction < 1000 kDa.

[32] The ratio [Excess L]/[Fe] (Figure 8 and Table 1) represents the relative saturation state of the ligands (cf. [Lt]/[Fe] ratio explained by *Thuróczy et al.* [2010, 2011]).

[33] The values of [Excess L]/[Fe] for each size fraction are shown in Figure 8. They were relatively high (~5–6) in the Barents Sea (St. 239), with a maximum at 25 m depth (~15). At St. 279 in the Kara Sea, the ratio values were relatively low (<1) between 25 and 50 m depth in the UNF

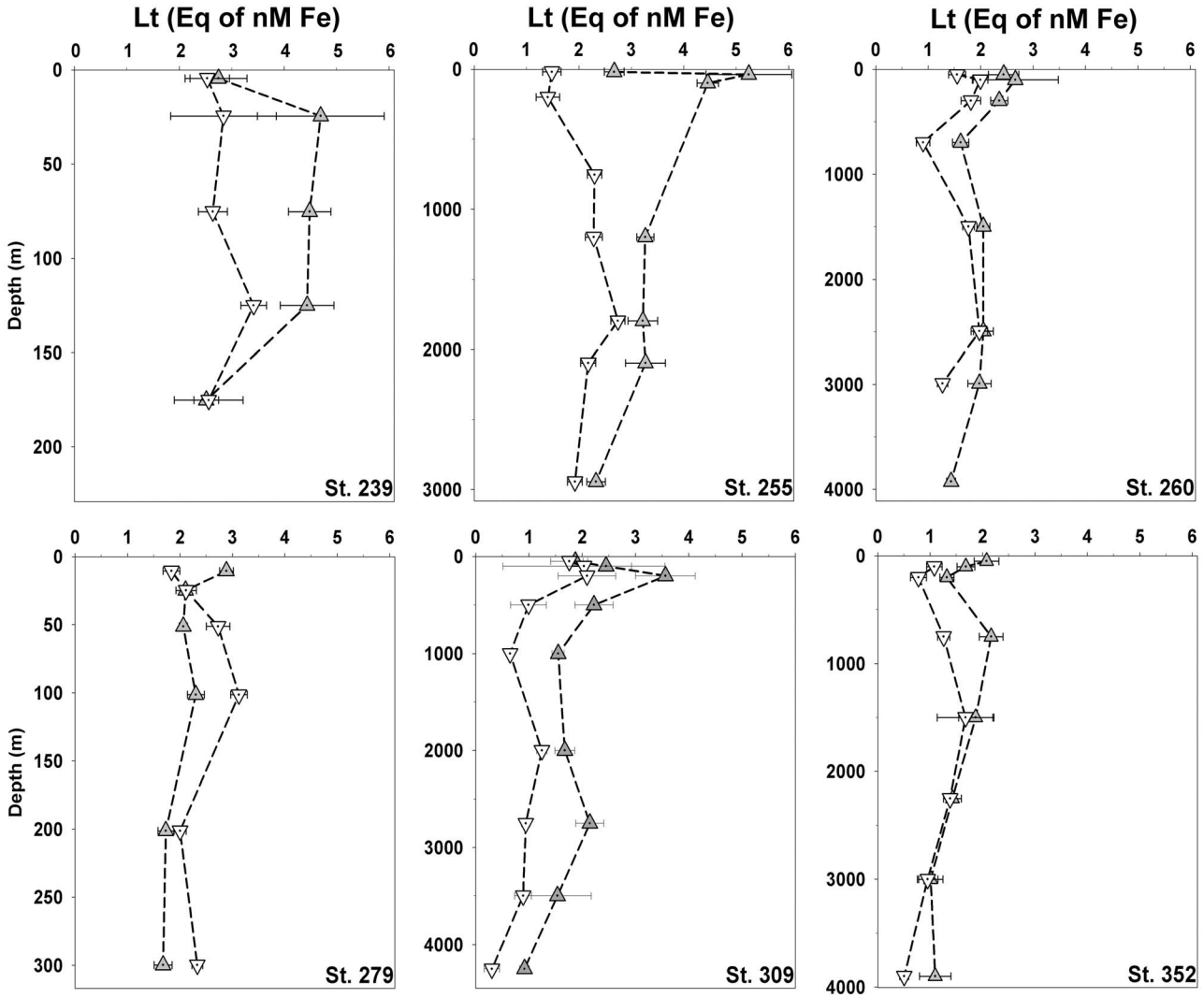

Figure 6b. Concentrations of Lt with depth at 6 stations sampled (same as in Figure 5) and for 2 size fractions: Dissolved fraction (<0.2 μm, gray triangles upwards looking) and fraction < 1000 kDa (white triangles downward looking). Ligand concentrations are in Eq of nM Fe (±standard deviation of the fit of the data to the model). Shelf sea stations are on the left side. The depth axes are extended until the bottom depth.

samples and dissolved fractions, whereas higher ratio values were present in the fraction < 1000 kDa (~4). The ratio [Excess L]/[Fe] in the Nansen Basin (St. 255 and 260) was high (>6) in the SW, decreasing with depth and remained low and relatively constant (~2–3) in deeper waters. Very low surface ratio values (<1) were seen in the Amundsen and Makarov basins (St. 309 and 352) where high Fe concentrations were measured at 50 m below the sea ice. Below the surface minimum in the Amundsen basin, high ratio values (>5) in the SW existed which decreased slightly with depth. In the fraction < 1000 kDa the ratio values were lower than in the dissolved fraction below 500 m depth. The Makarov Basin (St. 352) showed a reversed trend with depth, with a surface minimum (~0–1.5) and an increase of [Excess L]/[Fe] with depth in all size-fractions. The ratio values in the fraction < 1000 kDa were higher than those in the dissolved fraction and in UNF samples.

[34] Alpha, expressed here in its logarithm form ($\log_{10} \alpha$), is the product of K′ and Excess L. Alpha expresses the reactivity of the ligands. A high alpha favors Fe solubilzation via organic complexation (large Excess L, or high K′, or both). Reversely, a low alpha makes relatively easier the export and loss of Fe via precipitation and or scavenging. High alpha values were found on the slope of the Nansen Basin (St. 255, $\log\alpha$ > 13.5). Lower alpha values were found toward the central Arctic (at St. 309 in the Amundsen Basin and at St. 352 in the Makarov Basin, $\log\alpha$ < 13) (Table 1, 2a, and 2b and Figure 9).

4. Discussion

4.1. Iron Over the Different Fractions

[35] Large freshwater inputs from the Eurasian rivers bring organic matter, sediments and terrigenous materials

Table 1. Fe Concentrations, ±SD of Duplicate or Triplicate Measurements, and Ligand Characteristics for Two Size Fractions, ±SD of the Fit of the Data to the Langmuir Model[a]

Station	Fraction	Depth (m)	[Fe] (nM)	SD[b]	Ligand [Lt] (Eq of nM Fe)	SD	logK′ (mol^{-1})	SD	Sensitivity S ($A.mol^{-1}$)	SD	[Excess L] (Eq of nM Fe)	logα	pFe (M)	[Excess L]/ [Fe]
239, Barents Sea	<0.2 μm	5	0.408	0.036	2.75	0.54	21.94	0.29	0.98	0.09	2.34	13.31	22.70	5.7
		25	0.308	0.025	4.70	1.21	21.39	0.21	0.51	0.06	4.39	13.04	22.55	14.2
		75	1.051	0.002	4.49	0.41	21.81	0.08	1.02	0.07	3.44	13.35	22.33	3.3
		125	0.502	0.005	4.44	0.51	21.61	0.07	1.37	0.11	3.94	13.21	22.50	7.8
		175	0.486	0.017	2.51	0.24	21.69	0.09	1.63	0.06	2.03	12.99	22.31	4.2
	<1000 kDa	5	0.354	–	2.53	0.42	21.96	0.25	0.95	0.07	2.18	13.30	22.75	6.1
		25	0.241	0.004	2.84	1.01	21.49	0.20	0.89	0.15	2.60	12.91	22.53	10.8
		75	0.469	0.002	2.64	0.28	22.09	0.19	0.72	0.04	2.17	13.42	22.75	4.6
		125	0.391	0.011	3.42	0.25	22.47	0.21	0.79	0.04	3.03	13.96	23.36	7.7
		175	0.441	0.005	2.56	0.66	21.90	0.42	2.11	0.21	2.12	13.22	22.58	4.8
255, Nansen Slope	<0.2 μm	19	0.308	0.010	2.67	0.19	22.45	0.23	0.56	0.02	2.37	13.83	23.34	7.7
		37	0.430	0.030	4.26	0.50	21.93	0.13	0.39	0.04	3.83	13.51	22.88	8.9
		98	0.526	0.010	4.13	0.19	22.28	0.08	1.30	0.06	3.61	13.84	23.12	6.9
		200	0.556	0.020	ND	ND	ND	ND	ND	ND	ND	ND	ND	ND
		754	0.587	0.010	ND	ND	ND	ND	ND	ND	ND	ND	ND	ND
		1198	0.882	0.011	3.27	0.16	22.30	0.12	1.36	0.04	2.38	13.68	22.74	2.7
		1796	0.855	0.020	3.22	0.28	22.37	0.24	0.66	0.04	2.36	13.75	22.81	2.8
		2096	1.300	0.020	3.27	0.38	21.96	0.13	0.60	0.05	1.97	13.25	22.14	1.5
		2944	0.860	0.030	2.33	0.18	22.15	0.16	1.24	0.04	1.47	13.31	22.38	1.7
	<1000 kDa	19	0.230	0.000	1.48	0.18	22.18	0.28	1.39	0.04	1.25	13.27	22.91	5.5
		37	0.190	0.000	ND	ND	ND	ND	ND	ND	ND	ND	ND	ND
		98	0.440	0.000	ND	ND	ND	ND	ND	ND	ND	ND	ND	ND
		200	0.490	0.010	1.41	0.22	22.49	0.31	0.66	0.04	0.92	13.45	22.76	1.9
		754	0.493	0.023	2.30	0.14	22.18	0.13	0.73	0.02	1.80	13.43	22.74	3.7
		1198	0.530	0.030	2.28	0.16	22.08	0.13	0.61	0.02	1.75	13.33	22.60	3.3
		1796	0.757	0.078	2.74	0.13	22.36	0.12	1.43	0.04	1.99	13.65	22.78	2.6
		2096	0.600	0.020	2.16	0.14	21.97	0.08	1.10	0.03	1.56	13.16	22.38	2.6
		2944	0.640	0.010	1.92	0.14	22.36	0.23	0.79	0.02	1.28	13.47	22.66	2.0
260, Nansen Basin	<0.2 μm	50	0.274	0.027	2.44	0.29	21.64	0.11	1.02	0.04	2.17	12.98	22.54	7.9
		100	0.277	0.035	2.66	0.82	21.15	0.15	1.39	0.11	2.39	12.53	22.09	8.6
		300	0.512	0.007	2.36	0.16	22.27	0.17	0.81	0.03	1.84	13.53	22.82	3.6
		698	0.514	0.006	1.62	0.16	21.84	0.12	2.04	0.05	1.11	12.88	22.17	2.1
		1497	0.578	0.034	2.05	0.12	22.56	0.27	0.93	0.02	1.47	13.73	22.97	2.5
		2494	0.946	0.010	2.05	0.19	22.08	0.15	1.54	0.05	1.11	13.13	22.15	1.2
		2991	0.667	0.012	1.98	0.22	21.87	0.15	2.30	0.08	1.31	12.99	22.16	2.0
		3926	0.640	–	1.44	0.09	22.17	0.13	2.07	0.03	0.80	13.07	22.26	1.2
	<1000 kDa	50	0.138	0.006	1.55	0.16	22.23	0.25	0.68	0.02	1.41	13.38	23.24	10.2
		100	0.275	0.036	2.00	0.14	22.04	0.13	0.87	0.02	1.72	13.27	22.83	6.3
		300	0.346	0.002	1.82	0.19	22.10	0.21	0.92	0.03	1.47	13.26	22.72	4.2
		698	0.433	0.022	0.90	0.13	21.77	0.16	2.13	0.04	0.47	12.44	21.81	1.1
		1497	0.418	0.007	1.77	0.11	22.32	0.18	0.76	0.02	1.35	13.45	22.83	3.2
		2494	0.648	0.017	1.98	0.16	22.24	0.15	0.78	0.03	1.33	13.36	22.55	2.1
		2991	0.561	0.003	1.27	0.10	22.11	0.09	1.34	0.04	0.71	12.96	22.22	1.3
		3926	0.550	–	ND	ND	ND	ND	ND	ND	ND	ND	ND	ND
279, Kara Sea	<0.2 μm	11	0.887	0.008	2.89	0.13	21.79	0.05	1.16	0.02	2.00	13.09	22.14	2.3
		25	1.102	0.007	2.11	0.08	22.10	0.08	1.67	0.02	1.00	13.10	22.06	0.9
		51	1.326	0.005	2.06	0.08	22.46	0.13	1.69	0.03	0.74	13.33	22.21	0.6
		101	0.733	0.008	2.30	0.16	21.79	0.08	2.10	0.05	1.57	12.99	22.12	2.1
		201	0.631	0.002	1.73	0.15	21.94	0.13	1.63	0.04	1.10	12.98	22.18	1.7
		300	0.802	0.013	1.68	0.17	21.87	0.15	1.90	0.05	0.88	12.82	21.91	1.1
	<1000 kDa	11	0.537	0.016	1.84	0.16	22.05	0.16	0.99	0.03	1.30	13.16	22.43	2.4
		25	0.444	0.004	2.12	0.19	22.23	0.22	1.13	0.04	1.67	13.45	22.81	3.8
		51	0.572	0.017	2.73	0.22	22.00	0.13	1.01	0.04	2.16	13.34	22.58	3.8
		101	0.630	0.004	3.13	0.16	22.04	0.09	1.31	0.04	2.50	13.44	22.64	4.0
		201	0.539	0.017	2.00	0.12	22.25	0.14	0.89	0.02	1.46	13.42	22.69	2.7
		300	0.790	0.001	2.33	0.10	22.21	0.10	1.07	0.02	1.54	13.40	22.50	2.0
309, Amundsen Basin	<0.2 μm	50	1.444	0.030	1.87	0.14	22.57	0.33	0.82	0.03	0.43	13.21	22.05	0.3
		101	0.448	0.004	2.45	0.48	21.45	0.11	1.94	0.14	2.00	12.75	22.10	4.5
		201	0.407	0.006	2.74	0.39	21.60	0.09	2.76	0.14	2.33	12.97	22.36	5.7
		501	0.403	0.010	2.22	0.36	21.35	0.10	2.26	0.09	1.82	12.61	22.01	4.5
		1001	0.294	–	1.55	0.11	21.85	0.10	2.34	0.04	1.26	12.95	22.48	4.3

Table 1. (continued)

Station	Fraction	Depth (m)	[Fe] (nM)	SD[b]	Ligand [Lt] (Eq of nM Fe)	SD	logK′ (mol^{-1})	SD	Sensitivity S ($A.mol^{-1}$)	SD	[Excess L] (Eq of nM Fe)	logα	pFe (M)	[Excess L]/[Fe]
		2001	0.336	0.000	1.68	0.18	21.41	0.08	2.31	0.05	1.34	12.54	22.01	4.0
		2750	0.559	0.019	2.14	0.26	21.76	0.14	2.65	0.10	1.59	12.96	22.21	2.8
		3499	0.325	0.006	1.54	0.64	21.18	0.25	2.11	0.13	1.21	12.27	21.75	3.7
		4251	0.223	0.012	0.92	0.09	22.01	0.16	2.17	0.03	0.69	12.85	22.51	3.1
	<1000 kDa	50	0.927	0.026	1.76	0.35	22.04	0.36	1.64	0.12	0.83	12.96	21.99	0.9
		101	0.272	0.039	2.21	1.12	21.03	0.24	2.03	0.19	1.94	12.32	21.88	7.1
		201	0.239	0.003	2.09	0.54	21.16	0.11	2.34	0.12	1.85	12.43	22.05	7.7
		501	0.316	0.000	0.99	0.33	21.29	0.24	2.32	0.08	0.68	12.12	21.62	2.1
		1001	0.230	–	0.65	0.05	22.43	0.22	2.16	0.02	0.42	13.05	22.69	1.8
		2001	0.287	0.020	1.24	0.09	22.26	0.19	2.24	0.04	0.96	13.24	22.79	3.3
		2750	0.406	0.008	0.94	0.08	22.13	0.14	1.24	0.02	0.54	12.86	22.25	1.3
		3499	0.283	0.025	0.89	0.16	21.90	0.23	1.75	0.05	0.61	12.69	22.23	2.1
		4251	0.172	0.005	0.31	0.14	21.67	0.33	1.80	0.04	0.13	11.80	21.57	0.8
352, Makarov Basin	<0.2 μm	50	1.520	0.000	2.08	0.24	21.65	0.13	1.31	0.04	0.55	12.40	21.10	0.0
		100	0.651	0.018	1.68	0.17	21.85	0.12	1.08	0.04	1.03	12.87	22.05	1.6
		200	0.444	0.029	1.32	0.13	22.11	0.18	1.75	0.05	0.88	13.05	22.41	2.0
		751	0.451	0.009	2.16	0.23	21.71	0.11	1.50	0.05	1.71	12.94	22.29	3.8
		1500	0.330	0.006	1.87	0.32	21.47	0.13	1.95	0.05	1.54	12.66	22.14	4.7
		2251	0.241	0.013	1.43	0.17	21.77	0.14	1.79	0.04	1.19	12.84	22.46	4.9
		3001	0.167	0.002	1.01	0.23	21.69	0.28	1.90	0.06	0.85	12.62	22.40	5.1
		3900	0.219	0.010	1.10	0.30	21.61	0.31	1.85	0.08	0.88	12.55	22.21	4.0
	<1000 kDa	100	0.442	–	1.08	0.15	21.98	0.23	1.61	0.04	0.64	12.79	22.14	1.4
		200	0.310	0.011	0.78	0.15	21.76	0.25	1.64	0.04	0.47	12.43	21.94	1.5
		751	0.345	0.002	1.26	0.12	21.91	0.13	1.85	0.03	0.91	12.87	22.33	2.6
		1500	0.248	0.012	1.68	0.54	21.20	0.15	1.96	0.13	1.43	12.35	21.96	5.8
		2251	0.172	0.009	1.38	0.08	22.10	0.10	1.77	0.03	1.21	13.18	22.94	7.1
		3001	0.101	0.011	0.95	0.19	21.52	0.17	1.73	0.04	0.85	12.45	22.45	8.5
		3900	0.204	0.004	0.51	0.09	21.99	0.24	1.77	0.03	0.30	12.47	22.16	1.5
407, Laptev Sea	<0.2 μm	10	0.819	0.012	ND	ND	ND	ND	ND	ND	ND	ND	ND	ND
		30	0.715	0.009	2.15	0.28	21.57	0.12	1.24	0.04	1.43	12.73	21.88	2.0
		56	1.112	0.000	2.00	0.30	21.59	0.14	1.51	0.06	0.89	12.54	21.50	0.8
	<1000 kDa	10	0.698	0.029	ND	ND	ND	ND	ND	ND	ND	ND	ND	ND
		30	0.563	0.011	1.66	0.41	21.32	0.16	0.67	0.03	1.10	12.36	21.61	2.0
		56	1.004	0.027	1.96	0.25	21.58	0.10	0.75	0.02	0.96	12.56	21.56	1.0

[a]SD, standard deviation. Ligand characteristics are concentrations in Eq of nM Fe. The two size fractions are <0.2 μm and <1000 kDa. Conditional stability constants K′ are in mol^{-1}. S is the sensitivity of the titration measurement (slope of the straight part of the titration curve, in $Amp.mol^{-1}$). [Excess L] = [Lt]–[Fe]. Alpha = $\alpha_{organic}$ = [Excess L] · K′. pFe = -log {[Fe]/($\alpha_{inorganic}$ + $\alpha_{organic}$)}. ND, not determined.

[b]The standard deviation for Fe concentrations is missing when there were not enough samples to determine the concentration in duplicate or triplicate.

containing Fe toward the central Arctic. Part of these materials is trapped in the forming sea ice (Klunder et al., submitted manuscript, 2011a, 2011b) and transported away from the lands. During summer, this stock of Fe trapped in sea ice is released in seawater later in time and farther in place when melting occurs, and is responsible for the elevated concentrations of DFe (around 1.5 nM Fe, Figure 6a and Table 1) measured at the surface in the Amundsen and Makarov basins (St. 309 and 352, respectively) as also shown by Klunder et al. (submitted manuscript, 2011a, 2011b). This was also observed in the Southern Ocean by *Lannuzel et al.* [2007, 2008]. *Measures* [1999] also investigated the influence of sediments in sea ice on surface water Fe concentrations along a U.S.-Canadian section across the Arctic Ocean. He suggested that sediment trapped into sea ice may be of importance in transporting high Fe and Al concentrations to the surface waters of the central Arctic Ocean.

[36] *Wu et al.* [2001] showed that 30 to 70% of DFe in deep waters was present in colloidal form (between 0.02 and 0.4 μm). At all stations in our study, Fe concentrations in the fraction < 1000 kDa accounted for approximately 74 to 83% of the concentration of Fe in the dissolved fraction in the whole water column, thus 26 to 17% of DFe were present in the larger colloidal fraction (between 1000 kDa and 0.2 μm). Exception existed for the samples taken at the chlorophyll maximum where 42 to 64% of DFe was present in the fraction < 1000 kDa. These results showed that variations of the Fe pool in waters with phytoplankton activity was either due to the decrease (consumption) of Fe concentration in the smaller fraction (here <1000 kDa) and/or due to presence or formation of larger Fe colloids. *Boye et al.* [2010] also found in the Southern Polar Frontal Zone (between 20 and 21°E and 47.7–49.3°S) a significant portion (37 to 51%) of colloidal Fe (between 200 kDa and 0.2 μm) within the dissolved organic fraction.

[37] *Bergquist et al.* [2007] suggested that the variability of DFe (in <0.4 μm) was predominantly due to variations in the colloidal Fe as illustrated by the linear regression: $[Fe_{<0.4\ \mu m}] = 1.18\ [Fe_{0.02\ -0.4\ \mu m}] + 0.29$ ($R^2 = 0.85$). Similar results were found in the Eastern North Atlantic Ocean [*Thuróczy et al.*, 2010] using the same size fractions as in the present study ($[Fe_{<0.2\ \mu m}] = 1.16\ [Fe_{1000\ kDa-0.2\ \mu m}] + 0.03$;

Table 2a. Determination of the Ligand Characteristics in UNF Samples: Determination of an Upper Limit Using [TDFe]

Station	Depth (m)	[TDFe] (nM)	SD[a]	[Lt] (Eq of nM Fe)	SD	logK′ (mol^{-1})	SD	Sensitivity S ($A.mol^{-1}$)	SD	[Excess L] (Eq of nM Fe)	[Excess L]/ [TDFe]
239, Barents Sea	5	3.01	0.03	4.96	0.41	22.06	0.15	0.90	0.06	1.95	0.7
	25	3.61	0.01	7.23	0.22	22.26	0.06	1.14	0.05	3.62	1.0
	75	8.47	0.26	12.25	0.45	22.51	0.11	0.99	0.10	3.78	0.5
	125	54.79	0.54	56.93	0.11	23.66	0.08	1.06	0.03	2.14	0.0
	175	63.08	1.22	65.06	0.29	23.57	0.18	0.29	0.02	1.97	0.0
255, Nansen Slope	19	0.75	0.05	3.73	0.44	21.69	0.10	1.77	0.12	2.98	4.0
	37	1.16	0.06	ND	ND	ND	ND	ND	ND	ND	ND
	98	6.28	0.08	8.11	0.32	22.56	0.20	0.78	0.05	1.83	0.3
	200	6.54	0.08	ND	ND	ND	ND	ND	ND	ND	ND
	754	17.35	0.13	ND	ND	ND	ND	ND	ND	ND	ND
	1198	12.72	0.31	ND	ND	ND	ND	ND	ND	ND	ND
	1796	7.78	0.10	ND	ND	ND	ND	ND	ND	ND	ND
	2096	10.41	–	ND	ND	ND	ND	ND	ND	ND	ND
	2944	15.49	0.05	ND	ND	ND	ND	ND	ND	ND	ND
260, Nansen Basin	50	0.69	0.03	4.36	0.22	22.45	0.13	1.27	0.07	3.66	5.3
	100	0.95	0.01	3.01	0.23	22.27	0.19	1.27	0.05	2.05	2.2
	300	2.42	0.03	4.04	0.25	23.14	0.43	1.52	0.07	1.62	0.7
	698	2.91	0.06	4.33	0.17	22.66	0.23	0.93	0.03	1.42	0.5
	1497	3.68	0.18	4.88	0.15	22.68	0.16	1.53	0.04	1.20	0.3
	2494	5.26	0.04	6.64	0.09	22.92	0.11	2.06	0.04	1.38	0.3
	2991	4.83	0.13	7.15	0.19	22.59	0.11	1.90	0.07	2.31	0.5
	3926	4.52	0.24	5.12	0.20	23.41	0.39	0.71	0.03	0.60	0.1
279, Kara Sea	11	6.12	0.02	8.30	0.18	22.48	0.08	1.70	0.05	2.19	0.4
	25	5.04	–	6.01	0.08	23.19	0.17	1.26	0.02	0.96	0.2
	51	11.87	0.05	12.82	0.14	23.24	0.19	1.56	0.05	0.95	0.1
	101	8.48	0.07	9.42	0.11	23.16	0.15	1.46	0.03	0.94	0.1
	201	10.01	0.06	11.64	0.13	22.84	0.09	1.14	0.03	1.64	0.2
	300	11.00	–	12.26	0.39	22.82	0.29	0.67	0.05	1.26	0.1
309, Amundsen Basin	50	2.44	0.08	3.17	0.07	22.65	0.12	1.04	0.02	0.72	0.3
	101	2.39	0.01	4.81	0.48	21.68	0.08	1.82	0.12	2.42	1.0
	201	1.95	0.04	4.51	0.31	22.08	0.11	1.57	0.10	2.55	1.3
	501	1.80	0.05	3.27	0.21	21.93	0.10	1.71	0.06	1.47	0.8
	1001	3.50	0.09	4.12	0.13	22.47	0.13	1.59	0.04	0.62	0.2
	2001	2.83	0.05	4.73	0.38	21.83	0.10	1.83	0.10	1.90	0.7
	2750	3.52	0.09	4.91	0.28	22.27	0.14	2.48	0.11	1.39	0.4
	3499	4.25	0.08	5.86	0.34	22.56	0.28	1.98	0.12	1.61	0.4
	4251	2.66	0.01	3.23	0.08	22.70	0.15	1.73	0.03	0.57	0.2
352, Makarov Basin	50	1.61	0.06	2.74	0.44	21.60	0.16	1.32	0.07	1.13	0.7
	100	1.58	0.08	2.50	0.12	22.16	0.10	1.88	0.04	0.92	0.6
	200	1.10	0.04	2.05	0.14	21.95	0.11	1.65	0.04	0.95	0.9
	751	1.89	0.03	2.52	0.12	22.31	0.15	1.67	0.03	0.64	0.3
	1500	1.51	0.06	2.17	0.16	22.23	0.19	1.95	0.05	0.66	0.4
	2251	1.53	0.08	2.47	0.22	22.09	0.18	2.20	0.08	0.94	0.6
	3001	1.72	0.07	2.44	0.05	22.37	0.06	1.98	0.02	0.72	0.4
	3900	1.52	0.01	2.75	0.15	22.07	0.11	1.93	0.05	1.22	0.8

[a]The standard deviation for Fe concentrations is missing when there were not enough samples to determine the concentration in duplicate or triplicate.

R^2 = 0.93; n = 9). However, in the Arctic Ocean, no relationship was found between DFe and larger colloidal Fe, neither in the Atlantic sector of the Southern Ocean [Thuróczy, 2011]. Thus it appears that such a correlation is not applicable for all oceans. Further investigations are required here.

[38] *Nishioka and Takeda* [2000] have shown that colloidal Fe (between 200 kDa and 0.2 μm) was the most dynamic fraction during *Chaetoceros sp.* incubations and was consumed first, instead of soluble Fe (<200 kDa or <0.03 μm). Our results were consistent with their work; indeed, in the Barents Sea and Kara Sea, the concentration of Fe in the larger colloidal fraction (between 1000 kDa and 0.2 μm) was maximal at the fluorescence maximum (at about 40 m depth) and became smaller below this depth. Below 25 m in the Kara Sea (St. 279) and between 1000 and 3000 m in the Makarov Basin (St. 352), ligands in the dissolved fraction were more saturated than those in the fraction < 1000 kDa, meaning that ligands in the larger colloidal fraction (between 1000 kDa and 0.2 μm) were almost saturated. If colloids would aggregate, it would lead to a loss of Fe. *Wu et al.* [2001] showed that colloidal Fe (between 0.02 and 0.4 μm in their study) was important in removal processes when forming aggregates.

[39] The TDFe has been shown to be a good chemical tracer of physical processes in the oceans [*Takata et al.*, 2008; *Thuróczy et al.*, 2010]. By looking at Fe concentrations in UNF samples (TDFe), *Thuróczy et al.* [2010] could distinguish the Mediterranean Overflow Water in the Eastern North Atlantic Ocean. In the Amundsen Sea of the Southern Ocean, TDFe concentrations were still high (>30 nM Fe) up to 100 km away from the glaciers source and where the ligands were highly unsaturated with Fe in the dissolved fraction (Ratio [Lt]/[DFe] > 15), indicating solubilzation of Fe processes (L. J. A. Gerringa et al., Fe from melting glacier fuels the algal bloom in Pine Island Bay (Amundsen Sea, Southern Ocean), submitted to Deep-Sea Research, Part II, 2011; C.-E. Thuróczy et al., Key role of organic complex-

Table 2b. Determination of the Ligand Characteristics in UNF Samples: Determination of a Lower Limit Using [DFe]

Station	Depth (m)	[DFe] (nM)	SD[a]	[Lt][b] (Eq of nM Fe)	SD[b]	logK′[b] (mol^{-1})	SD[b]	Sensitivity S[b] ($A.mol^{-1}$)	SD[b]	[Excess L][b] (Eq of nM Fe)	[Excess L]/[DFe][b]
239, Barents Sea	5	0.41	0.04	3.46	1.40	21.38	0.25	1.02	0.18	3.05	7.5
	25	0.31	0.03	4.29	0.48	21.80	0.10	1.20	0.11	3.99	12.9
	75	1.05	0.00	4.99	0.72	21.92	0.15	1.00	0.14	3.94	3.8
	125	0.50	0.01	2.88	0.24	22.05	0.13	1.10	0.05	2.38	4.7
	175	0.49	0.02	2.50	0.33	21.93	0.22	0.29	0.02	2.02	4.2
255, Nansen Slope	19	0.31	0.01	4.00	0.57	21.48	0.08	1.94	0.15	3.69	12.0
	98	0.53	0.01	2.54	0.50	21.80	0.26	0.82	0.06	2.02	3.8
260, Nansen Basin	50	0.27	0.03	3.96	0.23	22.38	0.14	1.27	0.07	3.68	13.5
	100	0.28	0.04	2.70	0.34	21.91	0.16	1.34	0.08	2.43	8.8
	300	0.51	0.01	2.99	0.48	22.17	0.30	1.92	0.18	2.48	4.8
	698	0.51	0.01	1.99	0.24	22.17	0.29	0.94	0.04	1.48	2.9
	1497	0.58	0.03	2.15	0.24	21.86	0.15	1.61	0.06	1.57	2.7
	2494	0.95	0.01	2.43	0.11	22.28	0.11	2.09	0.04	1.49	1.6
	2991	0.67	0.01	3.30	0.30	21.97	0.12	1.99	0.11	2.64	4.0
	3926	0.64	–	1.24	0.22	22.74	0.44	0.71	0.03	0.60	0.9
279, Kara Sea	11	0.89	0.01	3.90	0.47	21.65	0.09	1.89	0.13	3.01	3.4
	25	1.10	0.01	2.07	0.09	22.66	0.21	1.26	0.02	0.97	0.9
	51	1.33	0.01	2.80	0.27	22.06	0.18	1.75	0.08	1.48	1.1
	101	0.73	0.01	1.92	0.19	22.11	0.16	1.51	0.04	1.18	1.6
	201	0.63	0.00	2.42	0.24	21.93	0.14	1.16	0.04	1.79	2.8
	300	0.80	0.01	2.91	0.53	21.67	0.16	0.75	0.06	2.11	2.6
309, Amundsen Basin	50	1.44	0.03	2.16	0.07	22.48	0.13	1.04	0.02	0.72	0.5
	101	0.45	0.00	–	–	–	–	–	–	–	–
	201	0.41	0.01	–	–	–	–	–	–	–	–
	501	0.40	0.01	2.52	0.60	21.39	0.16	1.87	0.14	2.12	5.3
	1001	0.29	–	1.64	0.75	21.19	0.28	1.70	0.12	1.34	4.6
	2001	0.34	0.00	–	–	–	–	–	–	–	–
	2750	0.56	0.02	1.17	0.16	21.93	0.18	1.99	0.06	0.62	1.1
	3499	0.32	0.01	–	–	–	–	–	–	–	–
	4251	0.22	0.01	0.88	0.17	21.79	0.26	1.74	0.04	0.66	3.0
352, Makarov Basin	50	1.52	0.00	2.70	0.46	21.57	0.16	1.33	0.07	1.17	0.8
	100	0.65	0.02	1.51	0.18	21.84	0.16	1.86	0.05	0.86	1.3
	200	0.44	0.03	1.89	0.32	21.43	0.13	1.74	0.06	1.45	3.3
	751	0.45	0.01	1.26	0.25	21.66	0.22	1.70	0.06	0.81	1.8
	1500	0.33	0.01	0.66	0.17	21.90	0.41	1.75	0.06	0.33	1.0
	2251	0.24	0.01	0.58	0.14	21.85	0.34	1.85	0.05	0.34	1.4
	3001	0.17	0.00	1.18	0.14	21.50	0.10	2.04	0.03	1.01	6.1
	3900	0.22	0.01	1.53	0.28	21.47	0.13	1.85	0.08	1.31	6.0

[a]The standard deviation for Fe concentrations is missing when there were not enough samples to determine the concentration in duplicate or triplicate.
[b]Values missing when the model could not fit the data using the lower limit.

ation of iron in sustaining phytoplankton blooms in the Pine Island and Amundsen Polynyas (Southern Ocean), submitted to *Deep-Sea Research, Part II*, 2011). In the present study, high concentrations of TDFe close to the sediment in the shelf seas resulted from the re-suspension of sediments. Similarly, the re-suspension of particles due to downslope processes were seen by elevated TDFe concentrations (St. 255, at 750 m depth) about 100 km away from the continental shelf of the Nansen Basin. A distinct maximum in [TDFe]/[DFe] (ratio value of 30) was found at the same location likely due to slope processes with sediment re-suspension and a relative enrichment of particulate Fe. These high TDFe concentrations at the Nansen Slope (St. 255) were matched with high concentrations of Mn [*Middag et al.*, 2009] and lower light transmission (Figure 4). These 3 studies suggest a horizontal transport of particles as already demonstrated by *Lam et al.* [2006], *Lam and Bishop* [2008], and *Raiswell et al.* [2008] in other oceans.

4.2. Complexation of Fe

4.2.1. In Surface Waters

[40] In surface waters, the observed high ligand concentrations can be caused by input of organic matter from rivers as previously reported by *Gerringa et al.* [2007] in the Scheldt estuary, and from the sea ice formed on the continental shelves. Sea ice is a potential source of ligands to the surface water because it contains organic matter from the rivers and from microorganisms. The accumulation of dissolved organic matter within sea ice was found to be several orders greater than in surface oceanic water as previously reported by *Thomas et al.* [2001], *Carlson and Hansell* [2004], and *Riedel et al.* [2008]. However, we cannot make any conclusions on the sea ice sources since we could not sample in the vicinity of sea ice; our first sample were taken at 20 m (St. 255 on the slope of the Nansen Basin) or at 50 m in the deep basins (St. 260, 309 and 352). On the shelf seas, the high ligands concentrations could be due to sediment re-suspension as suggested by *Gerringa et al.* [2008] for the Kerguelen Plateau with samples taken close to the bottom. At the surface and underneath sea ice, living organisms play a role in the chemistry of Fe. On the one hand, Fe is taken up by most of the living organisms (phytoplankton, bacteria and viruses); on the other hand, their presence generate organic matter (faeces, dead algae), which is degraded and remineralized into possible Fe-binding-ligands. The high DFe concentrations found in surface waters of the central Arctic (St. 309 in the Amundsen Basin and St. 352 in the Makarov Basin) might

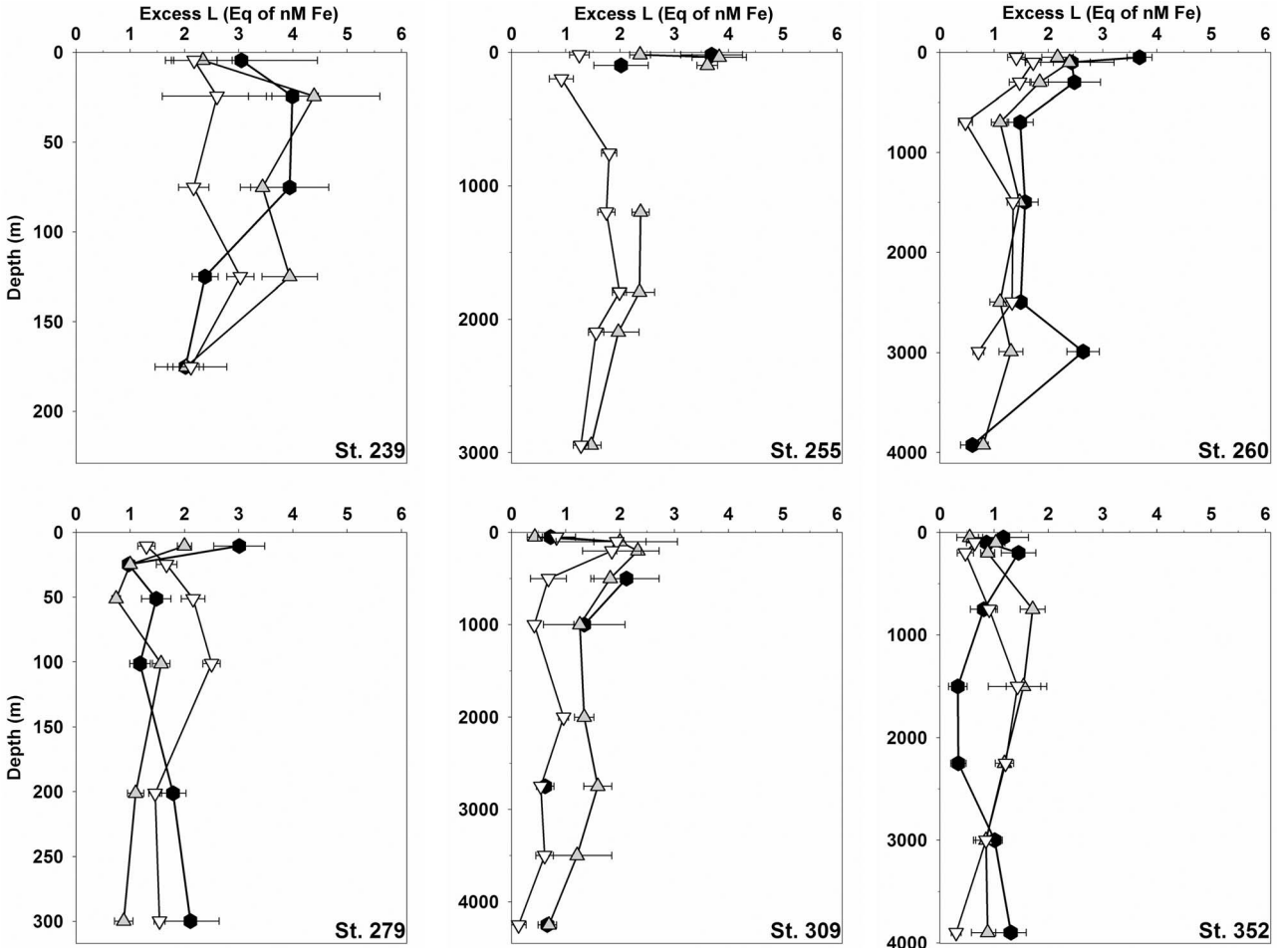

Figure 7. Excess L concentrations (Eq of nM Fe, ±standard deviation of the fit of the data to the model) with depth at 6 stations sampled (same as in Figure 5). Unfiltered samples using the lower limit (black dots), dissolved fraction (<0.2 μm; gray triangles upwards looking) and fraction < 1000 kDa; (white triangles downward looking). Shelf sea stations are on the left side. The depth axes are extended until the bottom depth.

have not been limiting for the phytoplankton [*Timmermans et al.*, 2005]. However, the thick layer of sea ice at the surface, source of Fe as discussed above, was most likely responsible for the lack of light leading to the low fluorescence recorded [*Timmermans et al.*, 2001, 2005]. Thus Fe uptake by biota should be small resulting in high DFe concentrations.

[41] In the surface waters of the Barents Sea (St. 239) and in the upper layer at the slope of the Nansen Basin (St. 255), relatively high Excess L and slightly weaker ligands (K′ value of $10^{21.39}$ and $10^{21.93}$, respectively, Table 1) were measured around the fluorescence maximum (fluorescence > 0.3 a.u., Figure 4). A possible explanation for relatively high Excess L concentrations and low conditional stability constant is the presence of exopolymer component like colloidal polysaccharide gels produced by organisms as found in Arctic sea ice by *Meiners et al.* [2008] and *Riedel et al.* [2007]. These colloidal polysaccharides present in relatively high concentration and with a relatively low binding constant [*Hassler et al.*, 2011; *Benner*, 2011] may behave as organic ligands thus having a pivotal role in the speciation of Fe in surface waters. Our results are also in line with the results of *Rijkenberg et al.* [2008] who suggested that ligands originating from phytoplankton, or at least found at the chlorophyll maximum, were relatively weak in contrast to ligands measured at larger depth. However, *Rue and Bruland* [1995] concluded that ligands originated from phytoplankton are stronger (relatively high K′ value). Stronger ligands were measured in the Nansen (St. 260) and Amundsen (St. 309) basins at the chlorophyll maximum; however, the fluorescence signal was lower here (<0.3 a.u.). Thus, there was no proof of a relation between phytoplankton and binding strength of ligands.

4.2.2. Saturation State of the Ligands and Scavenging of Fe

[42] The ratio [Excess L]/[Fe] (Figure 8) expresses the relative saturation of the ligands with Fe [*Thuróczy et al.*, 2010, 2011]. A high ratio means a relatively large excess of ligands, so an extra input of Fe would be easily complexed by the ligands. In this case, ligands have a high buffering capacity. A decrease in Fe also increases the ratio, and thus with respect to biota, an increasing ratio indicates depletion/consumption of Fe. A low ratio, approaching 0, indicates that the ligands become saturated and shows that

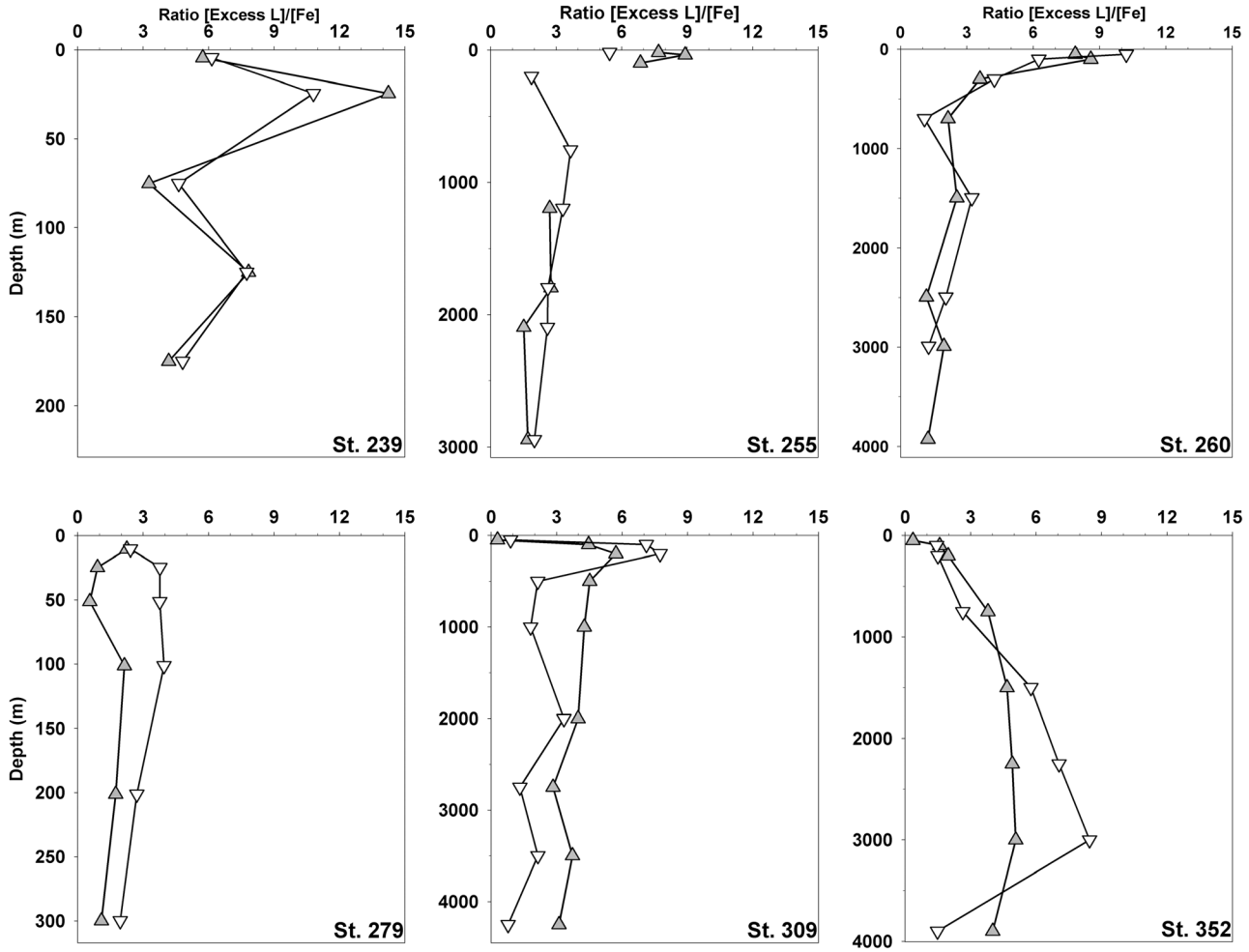

Figure 8. Ratio values [Excess L]/[Fe] for 6 stations sampled (same as in Figure 5) and for the 3 size fractions: Unfiltered samples using the lower limit (black dots), dissolved fraction (<0.2 μm; gray triangles upwards looking) and fraction < 1000 kDa; white triangles downward looking). A ratio of 0 means saturation of the ligands with Fe. Shelf sea stations are on the left side. The depth axes are extended until the bottom depth.

possible extra Fe inputs will be preferably removed by precipitation and/or scavenging. The ratio [Excess L]/[Fe] in the dissolved and <1000 kDa fractions decreased with depth, below the surface minimum in the Barents Sea and Amundsen Basin (St. 239 and 309, respectively), in all basins and seas with the exception of the Makarov basin. This decrease with depth was found in the Southern Ocean [*Thuróczy et al.*, 2011] and in the Eastern North Atlantic Ocean [*Thuróczy et al.*, 2010]. In both regions, below 450 m depth, low and constant values were found corresponding to relatively constant saturation state of the ligands. These results were supported by the work of *Boye et al.* [2010], who found an increasing portion of colloidal Fe (200 kDa-0.2 μm) as well as an increasing saturation of the ligands from the surface until 1000 m depth. In the deep waters (below 800 m) of the Nansen Basin (St. 260), the ratio [Excess L]/[Fe] was around 3, decreasing with depth. In the Amundsen Basin, the ratio was higher (3–5), showing that here the ligands were less saturated with Fe. Only the Makarov Basin (St. 352) showed the exact opposite trend with depth in the dissolved and <1000 kDa fractions, not yet found anywhere else [*Thuróczy et al.*, 2010, 2011]. The ratio values increased with depth (less saturation of the ligands with depth) indicating higher potential for Fe solubilzation. The increasing [Excess L]/[Fe] with depth in both dissolved and <1000 kDa fractions were caused by a larger decrease in Fe concentrations than Excess L concentrations. This revealed a possible loss of Fe and ligands toward the bottom as confirmed by increasing [TDFe]/[DFe] (Figure 10) indicating a the relative enrichment of particulate Fe and thus scavenging. Scavenging by settling particles is supported by the fact that the ligands are relatively weak and less reactive in the Makarov Basin compared to the Nansen and Amundsen basins (Figure 9). The combination of scavenging and a lack of Fe sources probably accounted for the net loss of DFe. This net loss was reflected by the increase in both [Excess L]/[Fe] and [TDFe]/[DFe].

4.2.3. Complexation of Fe in Unfiltered Samples

[43] The complexation of Fe in UNF samples is poorly described [*Nolting et al.*, 1998; *Thuróczy et al.*, 2010], certainly due to the uncertainty of the Fe concentration that is exchangeable. Part of Fe is refractory and irreversibly

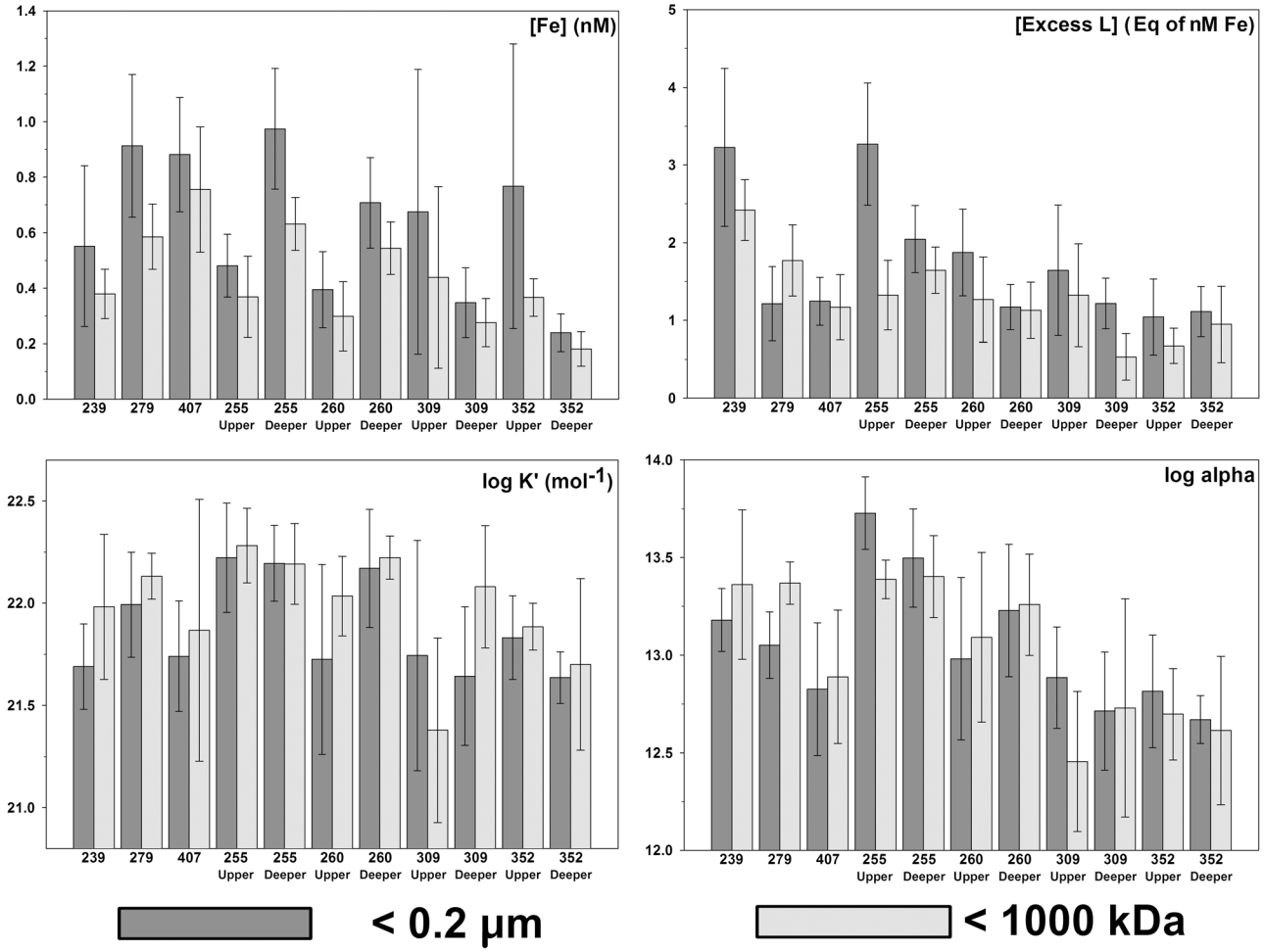

Figure 9. Average values (±Standard deviation) of Fe concentrations and ligand characteristics, for the dissolved fraction (<0.2 μm, dark gray) and fraction < 1000 kDa (light gray), at all the stations sampled, in the shelf seas (St. 239 in the Barents Sea, St. 279 in the Kara Sea and St. 407 in the Laptev Sea) and in the deep basins (St. 255 and 260 in the Nansen Basin, St. 309 in the Amundsen Basin and St. 352 in the Makarov Basin): in the upper basins (0–800 m, SW and AW) and in the deeper basins (below 800 m).

bound to particles or colloids under natural seawater conditions. The concentration of Fe used in the calculations influences the estimation of Lt and the strength K′. When TDFe is used, these parameters are overestimated; when DFe is used, they are possibly underestimated. However, Excess L is hardly changed when using different Fe concentrations in the calculation, therefore Excess L in UNF samples can be used as discussed by *Thuróczy et al.* [2010].

[44] Excess L concentrations in UNF samples were similar (within the standard deviations) to those in the smaller fraction at most of the stations indicating a small influence of the particulate fraction on the organic complexation of Fe, except in SW. In surface waters of the Nansen Basin (St. 255 and 260) and of the Kara Sea (St. 279), maximum Excess L in the UNF fraction (Tables 1, 2a, and 2b and Figure 7) were measured where Excess L was at minimum in the dissolved and <1000 kDa fractions. Thus, the largest excess of ligands must come from the particulate fraction (>0.2 μm) suggesting that particles could easily bind Fe (reactive) resulting in low excess L. These particles most likely originated from the rivers and sediments, as seen by the low light transmission (Figure 4). In the Makarov Basin, Excess L concentrations in the UNF samples were lower than in the dissolved and <1000 kDa fractions at 1500 and 2250 m depth. This apparent artifact was found in the upper core of the deep waters, just below the limit between the AIW and the AW.

4.3. Distinct Trends in Fe and Ligands Characteristics

[45] General trends in Fe concentrations and ligand characteristics were observed (Figure 9). By averaging each parameter per environment and per layer: the shelf seas (St. 239, 279 and 407), the upper layer (0–800 m, layer composed of SW and AW) and the deeper layer (<800 m, layer composed of the deep waters, AIW, CBW and DMBW) of the basins (St. 255, 260, 309 and 352), trends could be distinguished.

[46] The concentrations of DFe and $Fe_{<1000\ kDa}$ became slightly lower in the deeper ocean toward the central Arctic in the Makarov Basin (Figures 6a, 6b, and 9), as also shown by Klunder et al. (submitted manuscript, 2011a, 2011b). They showed that less Fe sources are present in the Makarov

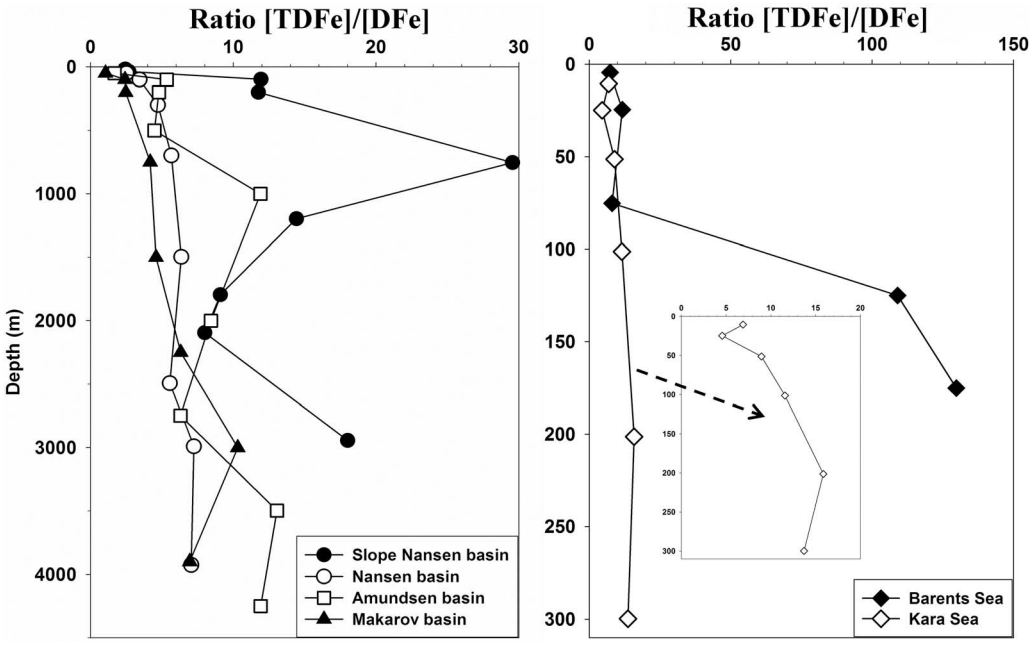

Figure 10. Ratio [TDFe]/[DFe] with depth. Graphs on the left are the deep basin stations (St. 255, 260, 309 and 352) and graphs at the right are the shelf sea stations (St. 239 and 279). Note the different scales for the ratio values and for the depths. The station in the Kara Sea is also enlarged (axis of the ratio until 20).

Basin compared to Amundsen Basin and Nansen Basins. The TDFe showed the same geographical trend as DFe (Figure 5): toward the central Arctic, TDFe decreased, from 3 to 6 nM Fe in the Nansen Basin, to 3 nM Fe in the Amundsen Basin and to 2 nM Fe in the Makarov Basin. This decrease of the particulate fraction toward the central Arctic is related to increasing distance from the shelf and slope sources and thus increasing time for removal processes (export of Fe) such as scavenging. The Deep Makarov Basin Water (DMBW) had different water properties (seen with θ/S diagrams, Figure 3) influenced by water from the Pacific Ocean which most likely explained the different ligand characteristics in deep waters of the Nansen and Amundsen basins (AW, AIW and CBW) and of the Makarov Basin (AW, AIW, CBW and DMBW).

[47] *Rue and Bruland* [1995] and *Buck and Bruland* [2007] investigated Fe and ligands in the Central North Pacific Ocean and in the Bering Sea, respectively, and could distinguish two classes of ligands using a different method as the one used in our study. They measured high Excess L concentrations (up to 1.8 Eq of nM Fe) in the surface samples increasing with depth to 2 Eq of nM Fe at 2000 m [*Rue and Bruland*, 1995], together with lower binding strength at depth. Excess L in our dissolved and <1000 kDa fractions were similar to their values, decreasing from 1.54 and 1.43 Eq of nM Fe, respectively, at 1500 m depth in the DMBW to 0.88 and 0.30 Eq of nM Fe at 3900 m depth, respectively. The ligands were also weaker in the DMBW than in the the upper waters. Overall this suggests the Pacific origin of the ligands in the DMBW.

[48] In the Amundsen and Makarov Basins, Excess L concentrations were lower than in the Nansen Basin (Figure 9). Trends in the binding strength were not obvious; slightly lower values were measured in the Amundsen and Makarov basins compared to the Nansen Basin (Table 1 and Figure 9). However, considering the stations in the basins, a distinct geographic trend existed in the alpha values (K′*Excess L), which expresses the reactivity of the ligands. Alpha clearly decreased from the continental slope (Figure 9, St. 255, logα > 13.5) toward the central Arctic Ocean (St. 352, logα < 13). This decrease in the reactivity of the ligands toward the central Arctic means higher potential for Fe export toward the seafloor in the Makarov Basin. But does alpha alone control the fate of Fe?

[49] The decrease of alpha in deep waters (below 800 m) toward the central Arctic Ocean fitted the increasing trends of the ligands saturation state (ratio [Excess L]/[Fe]) in the dissolved and <1000 kDa fractions. Ligands were more saturated with Fe (ratio [Excess L]/[Fe] < 3) where they were more reactive (higher alpha value) in the Nansen Basin (St. 260). In the Amundsen Basin, they were less saturated (ratio between 3 and 5) where they were less reactive. In the Makarov Basin, the ligands became unsaturated toward the bottom (ratio between 4 and 8) together with a decrease of their reactivity. As mentioned earlier, the decrease of the particulate fraction toward the central Arctic is related to increasing distance from the shelf and slope sources. Ligands can buffer Fe inputs but can also give away Fe when scavenging via sinking particles occurs. In the Nansen Basin where the ligands are reactive, the permanent Fe inputs, which lead to saturate the ligands with Fe, is larger than scavenging and removal processes. Conversely, in the deep Makarov Basin where the ligands are less reactive and where the sources of Fe are limited (Klunder et al., submitted manuscript, 2011a, 2011b), scavenging of Fe lead to the desaturation of the ligands and to a net export of Fe toward the seafloor because the flux of particles is apparently much larger than the flux of DFe. This highlights the

combination of little source of Fe and increasing time for scavenging toward the Makarov Basin.

[50] Trends existed between the seas, with decreasing alpha, decreasing Fe and increasing ratio [Excess L]/[Fe] from the Barents Sea (St. 239), Kara Sea (St. 279) toward the Laptev Sea (St. 407). This Eastward trend could be due to a dilution of the AW inflow on the shelves, and higher influence from the rivers.

5. Summary and Conclusions

[51] Our study presented the first data set on the complexation and size fractionation of Fe in the Arctic Ocean.

[52] Dissolved Fe (DFe) was for 74 to 83% present in the fraction < 1000 kDa, except at the chlorophyll maximum depth. Here, only 42 to 64% of DFe was present in the fraction < 1000 kDa, thus a somewhat larger portion of Fe in the larger colloidal fraction (between 1000 kDa and 0.2 μm). Distinct geographical trends in Fe and in ligands characteristics were seen from the shelf seas (Barents Sea) toward the central Arctic Ocean (Makarov Basin). In the surface waters and Atlantic waters (above 800 m depth), the concentrations of DFe and $Fe_{<1000\ kDa}$ were lower in the Nansen Basin (average [DFe] = 0.39 nM ± 0.14, n = 4; and average [$Fe_{<1000\ kDa}$] = 0.30 nM ± 0.12, n = 4) than in the Amundsen Basin (average [DFe] = 0.68 nM ± 0.51, n = 4; and average [$Fe_{<1000\ kDa}$] = 0.44 nM ± 0.33, n = 4) and in the Makarov Basin (average [DFe] = 0.77 nM ± 0.51, n = 4; and average [$Fe_{<1000\ kDa}$] = 0.37 nM ± 0.07, n = 3) as summarized in Figure 9. Below 800 m depth, higher concentrations of Fe were found in the Nansen Basin (average [DFe] = 0.71 nM ± 0.16, n = 4; and average [$Fe_{<1000\ kDa}$] = 0.54 nM ± 0.09, n = 4) compared to the Amundsen Basin (average [DFe] = 0.35 nM ± 0.13, n = 5; and average [$Fe_{<1000\ kDa}$] = 0.28 nM ± 0.09, n = 5) and in the Makarov Basin (average [DFe] = 0.24 nM ± 0.07, n = 4; and average [$Fe_{<1000\ kDa}$] = 0.18 nM ± 0.06, n = 4). A general decrease in excess of ligands (from approximately 3.5 to 1 Eq of nM Fe for the dissolved fraction, and from approximately 1.5 to 0.5 Eq of nM Fe for the fraction < 1000 kDa), and in the binding strength (logK' mainly >22 in the Nansen Basin, and logK' < 22 in the Amundsen and Makarov basins) resulted in a decrease in alpha. This corresponds to the ligand reactivity (average log α > 13.5 in the Nansen Basin, and <13 in the Amundsen and Makarov basins, Figure 9). Total dissolvable iron (TDFe) also decreased from the Nansen Basin where [TDFe] were above 3 nM Fe in the AW and EBDW, toward the Makarov basins where [TDFe] were lower than 2 nM Fe in the AW and DMBW. In addition, a relative enrichment of particulate Fe with depth at all stations was found looking at the ratio [TDFe]/[DFe], revealing removal of Fe via scavenging in the deep basins. Furthermore, in the Nansen and Amundsen basins, ligands in the dissolved and <1000 kDa fractions were more saturated with Fe with increasing depth (ratio [Excess L]/[Fe] decreasing from 13 at the surface to 1 at depth), which was related to more sources of Fe and to more reactive dissolved ligands (alpha > 13.5). Thus, Fe removal might be important here. Conversely, in the Makarov Basin, the dissolved ligands became desaturated with depth (ratio [Excess L]/[Fe] increasing from 0.4 at the surface to 8.5 at depth) as confirmed by their lower reactivity (alpha < 13). The Makarov Basin is far from large sources of Fe and ligands, thus increasing the time for scavenging and export of Fe. There, the flux of particles removing Fe is probably larger than the flux of DFe input leading to the desaturation of the ligands.

[53] To conclude, the reactivity (alpha value) and the saturation state (ratio [Excess L]/[Fe]) of the ligands proved to be excellent tools to explain the distribution and the fate of Fe in the different fractions when combining sources of Fe and ligands and removal processes like scavenging.

[54] **Acknowledgments.** The authors are very grateful to Captain S. Schwarze of Polarstern and his crew for their help and would like to thank Karel Bakker and Sven Ober from the Royal-NIOZ for the data of the nutrients and the CTD, respectively. Special thanks to Jun Nishioka for sharing his knowledge on using the 1000 kDa filters. This work was funded by the NWO. Geotraces sub-project 851.40.102, physical and chemical speciation of dissolved iron in polar oceans.

References

Anderson, L. G., G. Björk, O. Holby, E. P. Jones, G. Kattner, K. P. Koltermann, B. Liljeblad, R. Lindegren, B. Rudels, and J. H. Swift (1994), Water masses and circulation in the Eurasian Basin: Results from the Oden 91 expedition, *J. Geophys. Res.*, *99*(C2), 3273–3283, doi:10.1029/93JC02977.

Babin, M., A. Morel, and B. Gentili (1996), Remote sensing of sea surface Sun-induced chlorophyll fluorescence: Consequences of natural variations in the optical characteristics of phytoplankton and the quantum yield of chlorophyll a fluorescence, *Int. J. Remote Sens.*, *17*(12), 2417–2448, doi:10.1080/01431169608948781.

Benner, R. (2011), Loose ligands and available iron in the Ocean, *Proc. Natl. Acad. Sci. U. S. A.*, *108*, 893–894, doi:10.1073/pnas.1018163108.

Bergquist, B. A., J. Wu, and E. A. Boyle (2007), Variability in oceanic dissolved iron is dominated by the colloidal fratction, *Geochim. Cosmochim. Acta*, *71*(12), 2960–2974, doi:10.1016/j.gca.2007.03.013.

Boye, M., J. Nishioka, P. Croot, P. Laan, K. R. Timmermans, V. H. Strass, S. Takeda, and H. J. W. de Baar (2010), Significant portion of dissolved organic Fe complexes in fact is Fe colloids, *Mar. Chem.*, *122*, 20–27, doi:10.1016/j.marchem.2010.09.001.

Buck, K. N., and K. W. Bruland (2007), The physicochemical speciation of dissolved iron in the Bering Sea, Alaska, *Limnol. Oceanogr.*, *52*(5), 1800–1808, doi:10.4319/lo.2007.52.5.1800.

Carlson, C. A., and D. A. Hansell (2004), The contribution of DOM on the biogeochemistry of the Ross Sea, in *Biogeochemistry of the Ross Sea*, *Antarct. Res. Ser.*, vol. 78, edited by G. R. Di Tullio and R. B. Dunbar, pp. 123–142, AGU, Washington, D. C.

Croot, P. L., and M. Johanson (2000), Determination of iron speciation by cathodic stripping voltammetry in seawater using the competing ligand 2-(2-Thiazolylazo)-p-cresol (TAC), *Electroanalysis*, *12*(8), 565–576, doi:10.1002/(SICI)1521-4109(200005)12:8<565::AID-ELAN565>3.0.CO;2-L.

Cullen, J. T., B. A. Bergquist, and J. W. Moffett (2006), Thermodynamic characterization of the partitioning of iron between soluble and colloidal species in the Atlantic Ocean, *Mar. Chem.*, *98*(2–4), 295–303, doi:10.1016/j.marchem.2005.10.007.

de Baar, H. J. W., and J. T. M. de Jong (2001), Distributions, sources and sinks of iron in seawater, in *The Biogeochemstry of Iron in Seawater*, edited by D. R. Turner and K. A. Hunter, chap. 5, pp. 123–254, Wiley, Chichester, U. K.

de Baar, H. J. W., A. G. J. Buma, R. F. Nolting, G. C. Cadée, G. Jacques, and P. J. Tréguer (1990), On iron limitation of the Southern Ocean: Experimental observations in the Weddell and Scotia Seas, *Mar. Ecol. Prog. Ser.*, *65*(2), 105–122, doi:10.3354/meps065105.

de Baar, H. J. W., et al. (2008), Titan: A new facility for ultra-clean sampling of trace elements and isotopes in the deep oceans in the international Geotraces program, *Mar. Chem.*, *111*(1–2), 4–21, doi:10.1016/j.marchem.2007.07.009.

de Jong, J. T. M., J. den Das, U. Bathmann, M. H. C. Stoll, G. Kattner, R. F. Nolting, and H. J. W. de Baar (1998), Dissolved iron at subnanomolar levels in the Southern Ocean as determined by ship-board analysis, *Anal. Chim. Acta*, *377*(2–3), 113–124, doi:10.1016/S0003-2670(98)00427-9.

Gerringa, L. J. A., P. M. J. Herman, and T. C. W. Poortvliet (1995), Comparison of the linear van den Berg/Ružić transformation and a non-linear fit of the Langmuir isotherm applied to Cu speciation data in the estuarine

environment, *Mar. Chem.*, *48*(2), 131–142, doi:10.1016/0304-4203(94)00041-B.

Gerringa, L. J. A., M. J. W. Veldhuis, K. R. Timmermans, G. Sarthou, and H. J. W. de Baar (2006), Co-variance of dissolved Fe-binding ligands with phytoplankton characteristics in the Canary Basin, *Mar. Chem.*, *102*(3–4), 276–290, doi:10.1016/j.marchem.2006.05.004.

Gerringa, L. J. A., M. J. A. Rijkenberg, H. T. Wolterbeek, T. G. Verburg, M. Boye, and H. J. W. de Baar (2007), Kinetic study reveals Fe-binding ligand, which affects the solubility of Fe in the Scheldt estuary, *Mar. Chem.*, *103*(1–2), 30–45, doi:10.1016/j.marchem.2006.06.002.

Gerringa, L. J. A., S. Blain, P. Laan, G. Sarthou, M. J. W. Veldhuis, C. P. D. Brussaard, E. Viollier, and K. R. Timmermans (2008), Fe-binding organic ligands near the Kerguelen Archipelago in the Southern Ocean (Indian sector), *Deep Sea Res., Part II*, *55*(5–7), 606–621, doi:10.1016/j.dsr2.2007.12.007.

Gledhill, M., and C. M. G. van den Berg (1994), Determination of complexation of iron(III) with natural organic complexing ligands in sea water using cathodic stripping voltammetry, *Mar. Chem.*, *47*(1), 41–54, doi:10.1016/0304-4203(94)90012-4.

Guay, C., and K. Falkner (1997), Barium as a tracer of Arctic halocline and river waters, *Deep Sea Res., Part II*, *44*(8), 1543–1569, doi:10.1016/S0967-0645(97)00066-0.

Hassler, C. S., E. Alasonati, C. A. Mancuso Nichols, and V. I. Slaveykova (2011), Exopolysaccharides produced by bacteria isolated from the pelagic Southern Ocean—Role in Fe binding, chemical reactivity, and bioavailability, *Mar. Chem.*, *123*(1–4), 88–98, doi:10.1016/j.marchem.2010.10.003.

Hirose, K. (2007), Metal-organic matter interaction: Ecological roles of ligands in oceanic DOM, *Appl. Geochem.*, *22*(8), 1636–1645, doi:10.1016/j.apgeochem.2007.03.042.

Hudson, R. J. M., R. L. Rue, and K. W. Bruland (2003), Modeling complexometric titrations of natural water samples, *Environ. Sci. Technol.*, *37*(8), 1553–1562, doi:10.1021/es025751a.

Kepkay, P. E. (1994), Particle aggregation and the biological reactivity of colloids, *Mar. Ecol. Prog. Ser.*, *109*(2–3), 293–304.

Kiefer, D. A. (1973), Chlorophyll a fluorescence in marine centric diatoms: Responses of chloroplasts to light and nutrient stress, *Mar. Biol. Berlin*, *23*(1), 39–46, doi:10.1007/BF00394110.

Klunder, M. B., P. Laan, R. Middag, H. J. W. de Baar, and J. van Ooijen (2011), Dissolved Fe in the Southern Ocean (Atlantic sector), *Deep Sea Res., Part II*, doi:10.1016/j.dsr2.2010.10.042.

Kuma, K., J. Nishioka, and K. Matsunaga (1996), Controls on iron(III) hydroxide solubility in seawater: The influence of pH and natural organic chelators, *Limnol. Oceanogr.*, *41*(3), 396–407, doi:10.4319/lo.1996.41.3.0396.

Lam, P. J., and J. K. B. Bishop (2008), The continental margin is a key source of iron to the HNLC North Pacific Ocean, *Geophys. Res. Lett.*, *35*(7), L07608, doi:10.1029/2008GL033294.

Lam, P. J., J. K. B. Bishop, C. C. Henning, M. A. Marcus, G. A. Waychunas, and I. Y. Fung (2006), Wintertime phytoplankton bloom in the subarctic Pacific supported by continental margin iron, *Global Biogeochem. Cycles*, *20*, GB1006, doi:10.1029/2005GB002557.

Lannuzel, D., V. Schoemann, J. de Jong, J. L. Tison, and L. Chou (2007), Distribution and biogeochemical behaviour of iron in the East Antarctic sea ice, *Mar. Chem.*, *106*(1–2), 18–32, doi:10.1016/j.marchem.2006.06.010.

Lannuzel, D., V. Schoemann, J. de Jong, L. Chou, B. Delille, S. Becquevort, and J. L. Tison (2008), Iron study during a time series in the western Weddell pack ice, *Mar. Chem.*, *108*(1–2), 85–95, doi:10.1016/j.marchem.2007.10.006.

Logan, B. E., U. Passow, A. L. Alldredge, H.-P. Grossart, and M. Simon (1995), Rapid formation and sedimentation of large aggregates is predictable from aggregation rates (half lives) of transparent exopolymer particles (TEP), *Deep Sea Res., Part II*, *42*(1), 203–214, doi:10.1016/0967-0645(95)00012-F.

Martin, J. H., R. M. Gordon, and S. E. Fitzwater (1991), The case for iron, *Limnol. Oceanogr.*, *36*(8), 1793–1802, doi:10.4319/lo.1991.36.8.1793.

Measures, C. I. (1999), The role of entrained sediments in sea ice in the distribution of aluminum and iron in the surface waters of the Arctic Ocean, *Mar. Chem.*, *68*(1–2), 59–70, doi:10.1016/S0304-4203(99)00065-1.

Meiners, K., C. Krembs, and R. Gradinger (2008), Exopolymer particles: Microbial hotspots of enhanced bacterial activity in Arctic fast ice (Chukchi Sea), *Aquat. Microb. Ecol.*, *52*, 195–207, doi:10.3354/ame01214.

Middag, R., H. J. W. de Baar, P. Laan, and K. Baker (2009), Dissolved aluminium and the silicon cycle in the Arctic Ocean, *Mar. Chem.*, *115*(3–4), 176–195, doi:10.1016/j.marchem.2009.08.002.

Millero, F. J. (1998), Solubility of Fe(III) in seawater, *Earth Planet. Sci. Lett.*, *154*(1–4), 323–329, doi:10.1016/S0012-821X(97)00179-9.

Moore, J. K., and O. Braucher (2008), Sedimentary and mineral dust sources of dissolved iron to the world ocean, *Biogeosciences*, *5*(3), 631–656, doi:10.5194/bg-5-631-2008.

Nishioka, J., and S. Takeda (2000), Change in the concentrations of iron in different size fractions during growth of the oceanic diatom *Chaetoceros sp.*: Importance of small colloidal iron, *Mar. Biol. Berlin*, *137*(2), 231–238, doi:10.1007/s002270000347.

Nishioka, J., S. Takeda, C. S. Wong, and W. K. Johnson (2001), Size-fractionated iron concentrations in the northeast Pacific Ocean: Distribution of soluble and small colloidal iron, *Mar. Chem.*, *74*(2–3), 157–179, doi:10.1016/S0304-4203(01)00013-5.

Nishioka, J., S. Takeda, H. J. W. de Baar, P. L. Croot, M. Boye, P. Laan, and K. R. Timmermans (2005), Changes in the concentration of iron in different size fractions during an iron enrichment experiment in the Southern Ocean, *Mar. Chem.*, *95*(1–2), 51–63, doi:10.1016/j.marchem.2004.06.040.

Nolting, R. F., L. J. A. Gerringa, M. J. W. Swagerman, K. R. Timmermans, and H. J. W. de Baar (1998), Fe(III) speciation in the high nutrient, low chlorophyll Pacific region of the Southern Ocean, *Mar. Chem.*, *62*(3–4), 335–352, doi:10.1016/S0304-4203(98)00046-2.

Powell, R. T., and J. R. Donat (2001), Organic complexation and speciation of iron in the South and Equatorial Atlantic, *Deep Sea Res., Part II*, *48*(13), 2877–2893, doi:10.1016/S0967-0645(01)00022-4.

Raiswell, R., L. G. Benning, M. Tranter, and S. Tulaczyk (2008), Bioavailable iron in the Southern Ocean: The significance of the iceberg conveyor belt, *Geochem. Trans.*, *9*, 7–15, doi:10.1186/1467-4866-9-7.

Reinthaler, T., H. van Aken, C. Veth, J. Aristegui, C. Robinson, P. J. L. R. Williams, P. Lebaron, and G. J. Herndl (2006), Prokaryotic respiration and production in the meso- and bathypelagic realm of the eastern and western North Atlantic basin, *Limnol. Oceanogr.*, *51*(3), 1262–1273, doi:10.4319/lo.2006.51.3.1262.

Riedel, A., C. Michel, M. Gosselin, and B. LeBlanc (2007), Enrichment of nutrients, exopolymeric substances and microorganisms in newly formed sea ice on the Mackenzie shelf, *Mar. Ecol. Prog. Ser.*, *342*, 55–67, doi:10.3354/meps342055.

Riedel, A., C. Michel, M. Gosselin, and B. LeBlanc (2008), Winter-spring dynamics in sea ice carbon cycling in the coastal Arctic Ocean, *J. Mar. Syst.*, *74*(3–4), 918–932, doi:10.1016/j.jmarsys.2008.01.003.

Rijkenberg, M. J. A., L. J. A. Gerringa, K. R. Timmermans, A. C. Fischer, K. J. Kroon, A. G. J. Buma, H. T. Wolterbeek, and H. J. W. de Baar (2008), Enhancement of the reactive iron pool by marine diatoms, *Mar. Chem.*, *109*(1–2), 29–44, doi:10.1016/j.marchem.2007.12.001.

Rudels, B., R. D. Muench, J. Gunn, U. Schauer, and H. J. Friedrich (2000), Evolution of the Arctic Ocean boundary current north of the Siberian Shelves, *J. Mar. Syst.*, *25*(1), 77–99, doi:10.1016/S0924-7963(00)00009-9.

Rue, E. L., and K. W. Bruland (1995), Complexation of iron(III) by natural organic ligands in the central North Pacific as determined by a new competitive ligand equilibration/adsorptive cathodic stripping voltammetric method, *Mar. Chem.*, *50*(1–4), 117–138, doi:10.1016/0304-4203(95)00031-L.

Scientific Committee on Oceanic Research (2006), GEOTRACES: An international study of the marine biogeochemical cycles of trace elements and their isotope—Science plan, *GEOTRACES Rep. 1*, Baltimore, Md.

Sunda, W. G. (2001), Bioavailability and bioaccumulation of iron in the sea, in *The Biogeochemistry of Iron in Seawater*, *IUPAC Ser. Anal. Phys. Chem. Environ. Syst.*, vol. 7, edited by D. R. Turner and K. A. Hunter, chap. 3, pp. 41–84, Wiley, Chichester, U. K.

Sunda, W. G., D. G. Swift, and S. A. Huntsman (1991), Low iron requirement for growth in oceanic phytoplankton, *Nature*, *351*(6321), 55–57, doi:10.1038/351055a0.

Takata, H., K. Kuma, Y. Isoda, S. Otosaka, T. Senjyu, and M. Minagawa (2008), Iron in the Japan Sea and its implications for the physical processes in deep water, *Geophys. Res. Lett.*, *35*, L02606, doi:10.1029/2007GL031794.

Thomas, D. N., H. Kennedy, G. Kattner, D. Gerdes, C. Gough, and G. S. Dieckmann (2001), Biogeochemistry of platelet ice: Its influence on particle flux under fast ice in the Weddell Sea, Antarctica, *Polar Biol.*, *24*(7), 486–496, doi:10.1007/s003000100243.

Thuróczy, C.-E. (2011), Physical and chemical speciation of Fe in the polar oceans, Ph.D. thesis, 206 pp., Rijksuniv. Groningen, Groningen, Netherlands.

Thuróczy, C.-E., L. J. A. Gerringa, M. B. Klunder, R. Middag, P. Laan, K. R. Timmermans, and H. J. W. de Baar (2010), Speciation of Fe in the Eastern North Atlantic Ocean, *Deep Sea Res., Part I*, *57*(11), 1444–1453, doi:10.1016/j.dsr.2010.08.004.

Thuróczy, C.-E., L. J. A. Gerringa, M. B. Klunder, P. Laan, and H. J. W. de Baar (2011), Observation of consistent trends in the organic complexa-

tion of dissolved iron in the Atlantic sector of the Southern Ocean, *Deep Sea Res., Part II*, doi:10.1016/j.dsr2.2011.01.002, in press.

Timmermans, K. R., M. S. Davey, B. van der Wagt, J. Snoek, R. J. Geider, M. J. W. Veldhuis, L. J. A. Gerringa, and H. J. W. de Baar (2001), Co-limitation by iron and light of *Chaetoceros brevis*, *C. dichaeta* and *C. calcitrans* (Bacillariophyceae), *Mar. Ecol. Prog. Ser.*, *217*, 287–297, doi:10.3354/meps217287.

Timmermans, K. R., B. van der Wagt, M. J. W. Veldhuis, A. Maatman, and H. J. W. de Baar (2005), Physiological responses of three species of marine pico-phytoplankton to ammonium, phosphate, iron and light limitation, *J. Sea Res.*, *53*(1–2), 109–120, doi:10.1016/j.seares.2004.05.003.

Tomczak, M., and J. S. Godfrey (1994), Arctic oceanography: The path of North Atlantic Deep Water, in *Regional Oceanography: An Introduction*, edited by M. Tomczak and J. S. Godfrey, chap. 7, pp. 83–104, Pergamon, Oxford, U. K.

Tortell, P. D., M. T. Maldonado, J. Granger, and N. M. Price (1999), Marine bacteria and biogeochemical cycling of iron in the oceans, *FEMS Microbiol. Ecol.*, *29*(1), 1–11, doi:10.1111/j.1574-6941.1999.tb00593.x.

Turner, D. R., K. A. Hunter, and H. J. W. de Baar (2001), Introduction, in *The Biogeochemistry of Iron in Seawater*, *IUPAC Ser. Anal. Phys. Chem. Environ. Syst.*, vol. 7, edited by D. R. Turner and K. A. Hunter, pp. 41–84, Wiley, Chichester, U. K.

Turoczy, N. J., and J. E. Sherwood (1997), Modification of the van den Berg/Ruzic method for the investigation of complexation parameters of natural waters, *Anal. Chim. Acta*, *354*(1–3), 15–21, doi:10.1016/S0003-2670(97)00455-8.

Wells, M. L., and E. D. Goldberg (1993), Colloid aggregation in seawater, *Mar. Chem.*, *41*(4), 353–358, doi:10.1016/0304-4203(93)90267-R.

Wells, M. L., G. J. Smith, and K. W. Bruland (2000), The distribution of colloidal and particulate bioactive metals in Narragansett Bay, RI, *Mar. Chem.*, *71*(1–2), 143–163, doi:10.1016/S0304-4203(00)00046-3.

Wu, J., and G. W. Luther III (1995), Complexation of Fe(III) by natural organic ligands in the Northwest Atlantic Ocean by a competitive ligand equilibration method and a kinetic approach, *Mar. Chem.*, *50*(1–4), 159–177, doi:10.1016/0304-4203(95)00033-N.

Wu, J., E. Boyle, W. Sunda, and L.-S. Wen (2001), Soluble and colloidal iron in the oligotrophic North Atlantic and North Pacific, *Science*, *293*(5531), 847–849, doi:10.1126/science.1059251.

Yamamoto-Kawai, M., N. Tanaka, and S. Pivovarov (2005), Freshwater and brine behaviours in the Arctic Ocean deduced from historical data of δ18O and alkalinity (1929–2002 A.D.), *J. Geophys. Res.*, *110*, C10003, doi:10.1029/2004JC002793.

H. J. W. de Baar, L. J. A. Gerringa, M. Klunder, P. Laan, and C.-E. Thuróczy, Royal Netherlands Institute for Sea Research, PO Box 59, 1790 AB Den Burg, Netherlands. (charles-edouard.thuroczy@nioz.nl)

M. Le Guitton, Centre for Estuarine and Marine Ecology, Netherlands Institute for Ecology, Royal Dutch Academy of Sciences, PO Box 140, 4400 AC Yerseke, Netherlands.